
Doctoral Dissertations

Student Theses and Dissertations

1974

An analytical and experimental study of the dynamic response of a press

Woosoon Bai

Follow this and additional works at: https://scholarsmine.mst.edu/doctoral_dissertations



Part of the [Mechanical Engineering Commons](#)

Department: Mechanical and Aerospace Engineering

Recommended Citation

Bai, Woosoon, "An analytical and experimental study of the dynamic response of a press" (1974). *Doctoral Dissertations*. 281.

https://scholarsmine.mst.edu/doctoral_dissertations/281

This thesis is brought to you by Scholars' Mine, a service of the Missouri S&T Library and Learning Resources. This work is protected by U. S. Copyright Law. Unauthorized use including reproduction for redistribution requires the permission of the copyright holder. For more information, please contact scholarsmine@mst.edu.

AN ANALYTICAL AND EXPERIMENTAL STUDY
OF THE DYNAMIC RESPONSE OF A PRESS

BY

WOOSON BAI, 1940 -
(Woosoon)

A

DISSERTATION

Presented to the Faculty of the Graduate School of the
UNIVERSITY OF MISSOURI - ROLLA

In Partial Fulfillment of the Requirements for the Degree
DOCTOR OF PHILOSOPHY
in
MECHANICAL ENGINEERING

1974

T 3039
93 pages
c.1

Advisor

Irvin Foster
Gene J. Lehnhoff

Charles J. Haue
C.R. Barber
A. J. Perico

243152

ABSTRACT

This dissertation presents a simplified mathematical model and computer simulation of the vertical motion of a press. The model is verified by comparing simulation results with actual field measurements.

Using this model, the computer simulation is then extended to study the dynamic response of a bolted press, one with loosened anchor bolts, and one which is isolated. Press performance, in terms of acceleration of the press, velocity of its foundation, and forces transmitted to the foundation, is analyzed in relation to the foundation mass and the stiffness of the isolators, where applicable. Comparative performances of the presses secured by the various methods are discussed.

ACKNOWLEDGEMENTS

The author wishes to express his sincere appreciation to Dr. J. Earl Foster, his research advisor, for help and guidance throughout his study at the University of Missouri - Rolla. He also extends his thanks to Dr. Terry F. Lehnhoff, his committee chairman, and the other members of his committee, Dr. Clark R. Barker, Dr. Charles J. Haas, and Dr. Anthony J. Penico, for their encouragement and advice. Dr. George B. Clark and the personnel of the Rock Mechanics and Explosives Research Center are very much appreciated for the financial support given during most of the author's tenure at UMR, for the use of their equipment, and for their continued help during this project. The author also wishes to acknowledge the generosity of Mr. Sheldon E. Young, President of Vibro-Dynamics Corporation, for providing the specific equipment and background information which made the experimental tests possible. Finally, the cooperation of the Schwitzer Division of the Wallace Murray Corporation in providing facilities for the field tests is greatly appreciated.

TABLE OF CONTENTS

	Page
ABSTRACT	ii
ACKNOWLEDGEMENTS	iii
LIST OF FIGURES.	vi
LIST OF SYMBOLS.	ix
LIST OF TABLES	xi
I. INTRODUCTION AND REVIEW OF LITERATURE	1
II. GENERAL DESCRIPTION OF PRESSES.	7
A. Structure	7
1. Frame	7
2. Slide	11
3. Drive System.	11
4. Die Set	11
B. Foundation.	13
C. Dynamic Excitation.	13
III. MATHEMATICAL MODEL AND COMPUTER SIMULATION.	15
A. Mass.	15
B. Stiffness	17
C. Basic Assumption.	19
D. Equations of Motion	21
E. Computer Simulation	25
IV. EXPERIMENTAL TESTS.	28
A. Tests	28
B. Results	32

Table of Contents (continued)	Page
V. EXTENDED SIMULATION STUDIES.46
A. The Effects of Varying the Foundation Mass of a Bolted Press46
B. The Effects of Loosened Anchor Bolts57
C. The Effects of Varying the Foundation Mass of a Press Resting on Isolators61
VI. RESULTS AND DISCUSSION73
VII. CONCLUSIONS AND RECOMMENDATIONS.77
BIBLIOGRAPHY79
VITA80
APPENDICES81
A. Table I.81
B. Table II82

LIST OF FIGURES

Figure		Page
1.	Diagrammatic Sketch of a Press	2
2.	Two Common Types of Presses.	9
3.	Sketch of a Press Die Set.	12
4.	Diagrammatic Sketch Showing Major Elements of the Mathematical Model of the Press.	16
5.	Force Versus Deflection Curves for Parts of a Press	18
6.	Variation of Shear Modulus of Dry Sand with Void Ratio, γ , and Confining Stress.	20
7.	Coefficient β for Rectangular Footings	20
8.	Free Body Diagram of the Major Press Elements.	22
9.	Sketch of the Slide Drive System	23
10.	Flow Chart Showing Major Steps in Performing Computer Calculations.	27
11.	Photograph of Press on which Field Measure- ments Were Taken	29
12.	Photograph of Instrumentation Used in the Field.	30
13.	Diagrammatic Arrangement of Instrumentation and Computers.	31
14.	Recorded Stamping Pulse.	33
15.	Schematic Diagram Showing Maximum Accelerations Recorded at Various Locations on the Press	35
16.	Acceleration Recording from the Crown.	36
17.	Acceleration Recording from the Bed.	38
18.	Frequency Spectrum of Signal Shown in Figure 17.	39
19.	Computer Simulation Showing Crown Acceleration	40

Figure	Page
20. Computer Simulation Showing Bed Acceleration.41
21. Measured Floor Velocity43
22. Computer Simulation Showing Floor Velocity.44
23. Simulation of a Bolted Press Showing Crown Displacement.48
24. Simulation of a Bolted Press Showing Bed Displacement.49
25. Simulation of a Bolted Press Showing Crown Acceleration.50
26. Simulation of a Bolted Press Showing Bed Acceleration.51
27. Simulation of a Bolted Press Showing Foundation Velocity52
28. Simulation of a Bolted Press Showing Force Transmitted to the Foundation53
29. Maximum Acceleration of a Bolted Press as a Function of Foundation Mass55
30. Maximum Foundation Velocity of a Bolted Press as a Function of Foundation Mass55
31. Maximum Dynamic Force Transmitted to the Foundation of a Bolted Press as a Function of Foundation Mass.56
32. Maximum Deflection of a Bolted Press as a Function of Foundation Mass56
33. Maximum Acceleration of a Press with Loosened Anchor Bolts as a Function of Foundation Mass59
34. Maximum Foundation Velocity of a Press with Loosened Anchor Bolts as a Function of Foundation Mass59
35. Maximum Dynamic Force Transmitted to the Foundation of a Press with Loosened Anchor Bolts as a Function of Foundation Mass.60

Figure	Page
36. Simulation of an Isolated Press Showing Crown Displacement.	62
37. Simulation of an Isolated Press Showing Bed Displacement.	63
38. Simulation of an Isolated Press Showing Crown Acceleration.	64
39. Simulation of an Isolated Press Showing Bed Acceleration.	65
40. Simulation of an Isolated Press Showing Foundation Velocity	66
41. Simulation of an Isolated Press Showing Force Transmitted to the Foundation	67
42. Maximum Acceleration of an Isolated Press as a Function of Foundation Mass	68
43. Maximum Foundation Velocity of an Isolated Press as a Function of Foundation Mass.	70
44. Maximum Dynamic Force Transmitted to the Foundation of an Isolated Press as a Function of Foundation Mass.	71

LIST OF SYMBOLS

a	Upper break point
b	Lower break point
c	Static deflection
d	Anchor bolt clearance
g	Acceleration of gravity
t	Time
A_F	Area of the underside of the foundation
C_1	Damping coefficient of soil
C_2	Damping coefficient between the bed and the foundation
C_3	Damping coefficient between the crown and the bed
F_S	Stamping force
F_B	Vertical component of the bearing reaction force
F_{CR}	Force in the connecting rod
G	Shear modulus
H_i	Fixed distance in Figure 9
K_1	Stiffness of soil
K_2	Stiffness between the bed and the foundation
K_3	Stiffness between the crown and the bed
K_{BT}	Stiffness of the anchor bolts
K_{CL}	Stiffness of the columns
K_{CN}	Stiffness of the effective concrete
K_{TR}	Stiffness of the tie rods
L	Length of the connecting rods
R	Length of the crank arm

List of Symbols (continued)

M_i	Mass of body i , $i = 1, 2, 3, 4$
Y_i	Displacement of body i from equilibrium position, $i = 1, 2, 3, 4$
\dot{Y}_i	Velocity of body i , $i = 1, 2, 3, 4$
\ddot{Y}_i	Acceleration of body i , $i = 1, 2, 3, 4$
Z	Vertical projection of the connecting rod L
α	Mass ratio of the foundation to the press
β	Coefficient
γ	Void ratio
ζ	Critical damping ratio
θ	Angle
$\dot{\theta}$	Angular velocity
$\ddot{\theta}$	Expressions in Equation (9)
ν	Poisson's ratio
σ_{cf}	Confining stress of soil

LIST OF TABLES

Table	Page
I. Specifications of the 60-Ton Press81
II. Specifications of the 600-Ton Press82

I. INTRODUCTION AND REVIEW OF LITERATURE

Research in the noise and vibration associated with factories has increased recently, parallel with a growing concern for human safety and operational efficiency. Machines and humans have to function harmoniously in a modern environment. Injury or physical discomfort to humans, however, as well as malfunction or failure of machine systems, can result from the dynamic excitation associated with the mechanical vibrations and high noise level of that environment.

Presses such as the one shown in Figure 1 are the major source of the vibration and noise related with most production operations. They cause a high level of acoustic noise which results in hearing damage, physical discomfort, and fatigue to the operator, as well as mechanical vibrations which result in damage to the press, its foundation, and the building.

In an attempt to regulate environments which are potentially harmful to workers, the 1970 Occupational Safety and Health Act and the 1969 Revision of the Walsh-Healey Public Contracts Act were passed. They define permissible noise exposure as 90 dB(A) for eight hours per day, with the exposure time reduced by one-half for

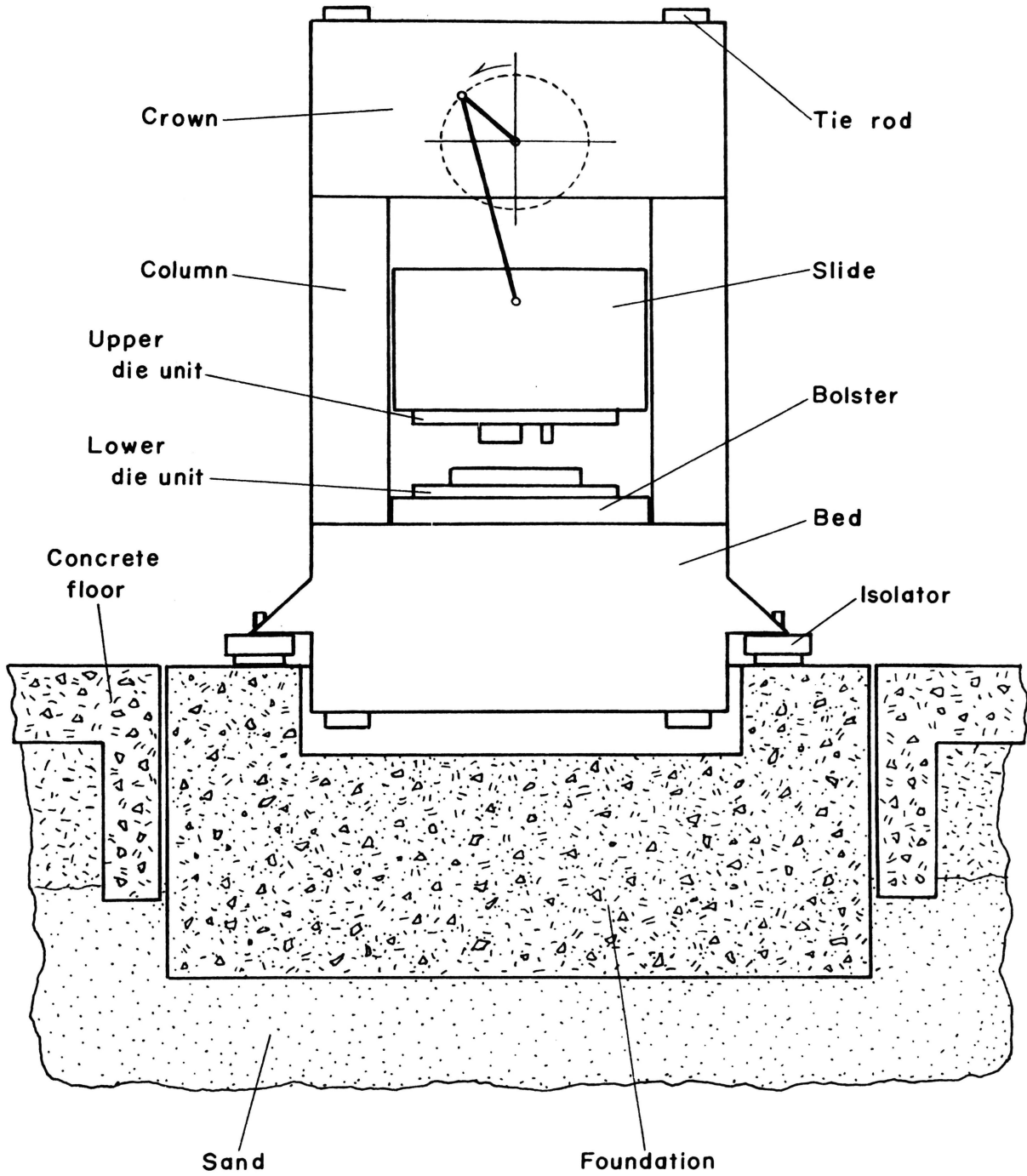


Figure 1. Diagrammatic Sketch of a Press

every 5 dB(A) increase above that level, up to a maximum of 115 dB(A) (1)*.

In general, all rotating and reciprocating machinery generates periodic forces due to the mass unbalance during its motion. A press, however, creates not only these periodic forces, but also direct impact forces during its stamping operation. This high-energy shock pulse imposes transient forces in addition to the usual harmonic forces exerted by the drive system.

There are three elements to be considered in controlling noise and vibration problems: the source, the pathway, and the receiver. It is common to deal with the pathway or the receiver only in cases of a high level of noise and vibration. This may involve such methods as enclosing the press in a separate room, or requiring the operator to wear a headset. However, the fundamental approach to the problem would be to eliminate or reduce the source as much as possible. This would not only lessen the damaging effects on the receiver, but would also reduce wear on the machine.

The noise level associated with the stamping operation of a typical press is directly affected by several parameters, such as operating speed, the material processed, its

*Numbers in parenthesis refer to the bibliography at the end of the dissertation.

thickness, and the type of process itself (e.g., blanking, forging, shearing, etc.). It has been reported that a 70 percent increase in machine speed increases the overall noise level five to ten dB, and that stamping of hard steel produces about five dB more noise than does stamping of mild steel (2). A reduction of dynamic excitation is, of course, one of the fundamental approaches to the noise and vibration problem. Unfortunately, however, this is not always possible. Reduction of the press's speed, for example, may not be economically feasible, while the nature and thickness of the material, as well as the type of process, are predetermined by the nature of the final product.

Rigidization of structural members of a press may increase its overall strength and decrease the level of noise. However, increasing the stiffness of a structural member, with a concurrent change in local mass, would produce new resonances which might result in other problems (3) A press having structural members made of cast iron may be superior to one with structural members made of welded plates, in terms of radiated noise. This is due to the importance of the role played by structural damping, and in one case led a press manufacturer to fill most of the voids in the structural members with scrap steel to help reduce radiated noise at the operator position.

The method of installing a press has been known to be an important factor associated with its performance and life, as well as with the life of the die set. Industries using presses have spent a great deal of money in developing installation methods which attempt to reduce the radiated and transmitted noise, and the transmission of dynamic excitation to the foundation and building. While isolators are widely used for the installation of presses on either a concrete floor or a concrete foundation, many manufacturers bolt their presses down tightly. The theory for the latter method states that the foundation absorbs the shock from the press, and that the foundation and anchor bolts hold the press securely in alignment (4).

It is important to consider the machine's foundation as one element of the vibratory system when studying noise and vibration control. Foundations for mounted equipment must be designed so that their lowest resonance frequencies are removed from the excitation frequencies of the equipment. The important parameters which control the performance of a machine's foundation are physical dimensions, stiffness, mass, and local characteristics at the points of equipment attachment (5), as well as the properties of the soil under the foundation.

Designers have held, until recently, that the amplitude of a machine's vibrations will decrease as the mass of its foundation is increased. For this reason, foundations

have been designed as massive blocks weighing several thousand tons and buried at depths approaching 30 or 40 feet (6). This is, obviously, a source of great expense to press users.

The objective of this paper is to formulate a mathematical model of the vertical motion of a press in order to understand and study the nature of the press's dynamic response, particularly as it relates to the noise and shock transmitted to its foundation, and to verify this model with actual data obtained by experimental tests carried out with a 60-ton press at a local manufacturing plant. Specific areas which will be studied by means of the mathematical model and computer simulation are the effects of varying the foundation mass, a comparison between the performance of a bolted press and that of one resting on isolators, and the effects of loosening the anchor bolts.

In order to formulate a mathematical model of a press, it is necessary to understand the structure and mechanism of presses to a certain extent. Therefore, the basic elements of a press will be discussed in the following chapter.

II. GENERAL DESCRIPTION OF PRESSES

Presses of one size or another are found in most manufacturing facilities, since they have a wide range of uses, such as cutting, forming, drawing, forging, stamping, etc. Their capacity varies from 40 to 2,000 tons, their speed from 20 to perhaps 1500 strokes per minute, and their stroke length from one-half to twelve inches. Most presses work vertically, although some of them are inclined or horizontal. Generally, presses consist of four basic elements: the frame, the slide (or ram), the driving system, and the die set.

A. Structure

1. Frame (7)--There are two types of frame: the "C" frame and the straight-sided frame. The former, as its name indicates, has one open side, while the latter has a contoured, rectangular shape. There are many types of presses which employ the "C" frame, since the open side of the frame results in fewer restrictions on press operations than does the closed, straight-sided frame. However, a press with a straight-sided frame can have a larger tonnage than can one with a "C" frame.

There are five types of "C" frame, as follows:

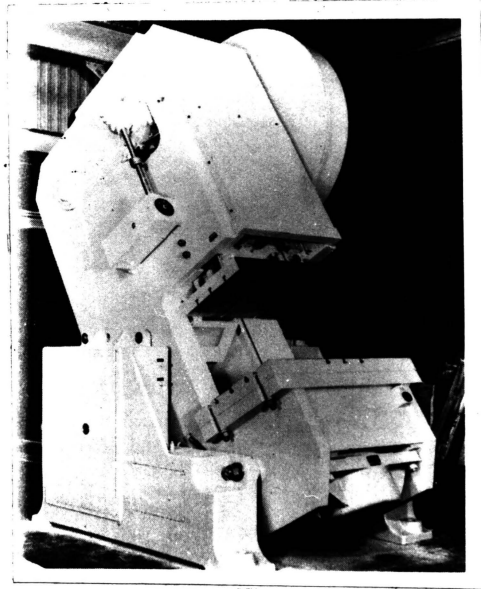
- a) Inclined, or open back inclined (OBI);
- b) Solid, or gap;
- c) Adjustable bed, or knee;

- d) Horning; and
- e) Open end, or endwheel.

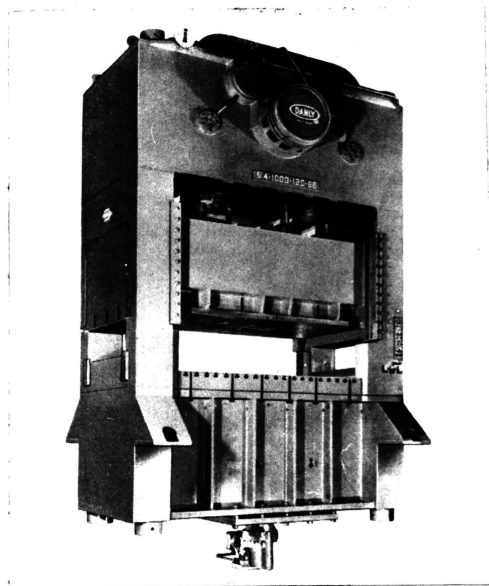
The inclinable press has special legs so that the frame can be inclined at three or four different angles. The main advantage of this type of press is its use of gravity to aid the passage of parts or scrap through the open back (see Figure 2(a)). The frame of a gap press is constructed as one permanently joined unit, so that it can be designed for higher tonnages than can inclinable presses. In an adjustable bed press, the lower part of the "C" frame contains a bed which can be adjusted to various heights. Although this press is limited to smaller tonnages, it has a relatively wide range of usage.

The horning press and the open end press have rather unusual features. The former has a large round post fitted into the vertical frame to handle tubular sheet metal. The latter has an open end on the bed.

The frame of a straight-sided press consists of a crown, two columns (or uprights), and a bed. The crown, which is the top side of the frame, usually contains the driving system for the stamping operation. The bed, which is the bottom side of the frame, has a bolster, similar to a table top, on which the die is mounted and which rests on four legs that support the whole press. The columns, which are the sides of the frame, have two guide rails containing bearings that support the slide and force it to maintain a reciprocating motion.



a) Inclined OBI Press (After Eary (7))



b) Tie-Rod Straight-Sided Press (After Eary (7))

Figure 2. Two Common Types of Press

There are four types of straight-sided frame, as follows:

- a) Solid;
- b) Arch;
- c) Pillar; and
- d) Tie rod.

The solid straight-sided frame is a box-shaped, single unit, and thus is the most rigid type of frame. However, shipment of this type of press is more difficult and, for this reason, there is an optimum limit on the tonnage or size of the press. The arch straight-sided frame is not commonly used. Its shape provides for larger bed areas.

The pillar straight-sided frame is used mainly for hydraulic construction. Four large, round pillars are fastened to the bed and the crown by retaining nuts which bear against a flange on the pillar ends. This type of press has the highest tonnage and is used in extrusion operations.

The tie rod straight-sided frame is the most common type of vertical press having a high tonnage. The crown, bed, and columns for this type of press are cast or welded as separate units. Four tie rods and the two columns separate the crown and the bed by a distance equal to the height of the columns, and are prestressed to a given percentage of the press's tonnage. The design is such that during the stamping operation there are no gaps in

the interfaces between the columns and the crown or bed. A typical tie rod straight-sided press is shown in Figure 2(b).

2. Slide (or Ram)--The slide is a massive block between the crown and the bed. It carries the punch, and is forced to follow a reciprocating motion by the bearings in the guide rails of the columns.

3. Drive System--There are two kinds of drive systems which power the slide to perform its operation: hydraulic and mechanical. A hydraulic drive system has a piston and slide as one unit, driven by an oil pump. Most mechanical drive systems consist of a crankshaft or eccentric, a flywheel, reduction gear trains, connecting rods, clutches, and a motor. Some mechanical drive systems, however, have racks and pinions or a heavy screw instead of crankshafts and connecting rods.

A hydraulic press can exert its full tonnage at any position of the slide stroke, and its stroke can be any length within the limits of the design of the hydraulic cylinder. In a mechanical press, however, full tonnage is available only at the bottom portion of the stroke, and the stroke length is constant.

4. Die Set (7)--A die set, in general, consists of four basic elements: the die, the punch, the stripper, and the guider (see Figure 3). The die (or female) steel, attached to the die shoe, is fastened to the

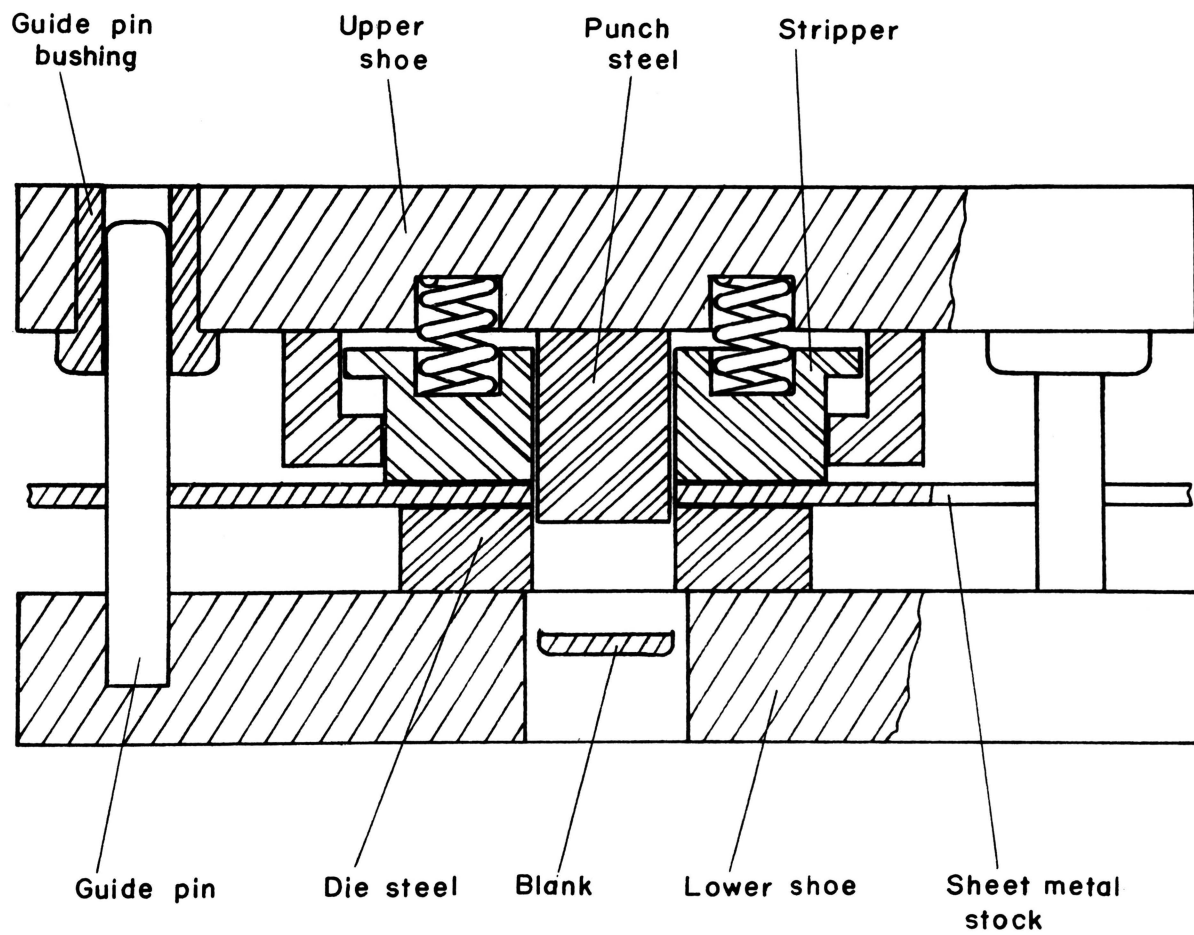


Figure 3. Sketch of a Press Die Set

bolster which, in turn, is mounted on the bed. The punch (or male) steel, attached to the punch shoe, is mounted under the slide.

The function of the stripper plate is to remove the sheet metal stuck to the punch steel after the punching operation. This phenomenon, called cold welding, is caused by the sliding action of the punch steel against the material under high pressure. It occurs particularly when cutting soft metals.

There is an optimum amount of clearance between the punch and the die cutting edges during the punching operation. This clearance is insured by means of guide pins and guide pin bushings.

B. Foundation

Most high performance presses have a heavy concrete block for a foundation, with a weight of roughly the same magnitude as the press. It is important to consider the machine's foundation as one element of the vibratory system when studying noise and vibration control (5).

C. Dynamic Excitation

The two sources of excitation of a press are the stamping force and the inertial loading by the drive system. During inertial loading, the press moves as a rigid body in phase with the reciprocating motions of the slide. It may not play as important a role as the stamping force at low speeds, but at higher speeds this force becomes significant.

The stamping force, which occurs near the bottom of the slide's stroke, is transmitted directly to the bed through the lower die and to the crown and the driving gear trains through the slide mass and the connecting rods. When the stamping starts, a relative displacement takes place between the crown and the bed. Free oscillations are triggered by the sudden release of potential energy stored in the tie rods and columns just at the end of the stamping operation. This impulsive force causes the acoustic radiation of the press, as well as the structural vibrations which are transmitted through the foundation as shock waves.

III. MATHEMATICAL MODEL AND COMPUTER SIMULATION

A tie rod straight-sided press has been chosen for the mathematical model because it is the most common type of high tonnage press, and because it is relatively simple to express in mathematical form. A three degree of freedom spring-mass system with damping has been employed for modelling the press with a foundation.

A. Mass

The total mass of the press with a foundation will be separated into four parts for the purposes of this paper, as shown in Figure 4: the crown, the bed, the slide, and the foundation.

The crown represents the lumped mass of the top frame, including the drive system, and of half of the side frame and the connecting rods. The bed is the sum of the masses of the bottom frame with the bolster and the lower part of the die set, and of the other half of the side frame. The slide is the sum of the masses of the sliding block with the upper part of the die set, and of the other half of the connecting rods. The foundation mass represents the concrete foundation block.

In later studies involving the foundation analysis, the mass will be varied from one-fifth to ten times the press mass.

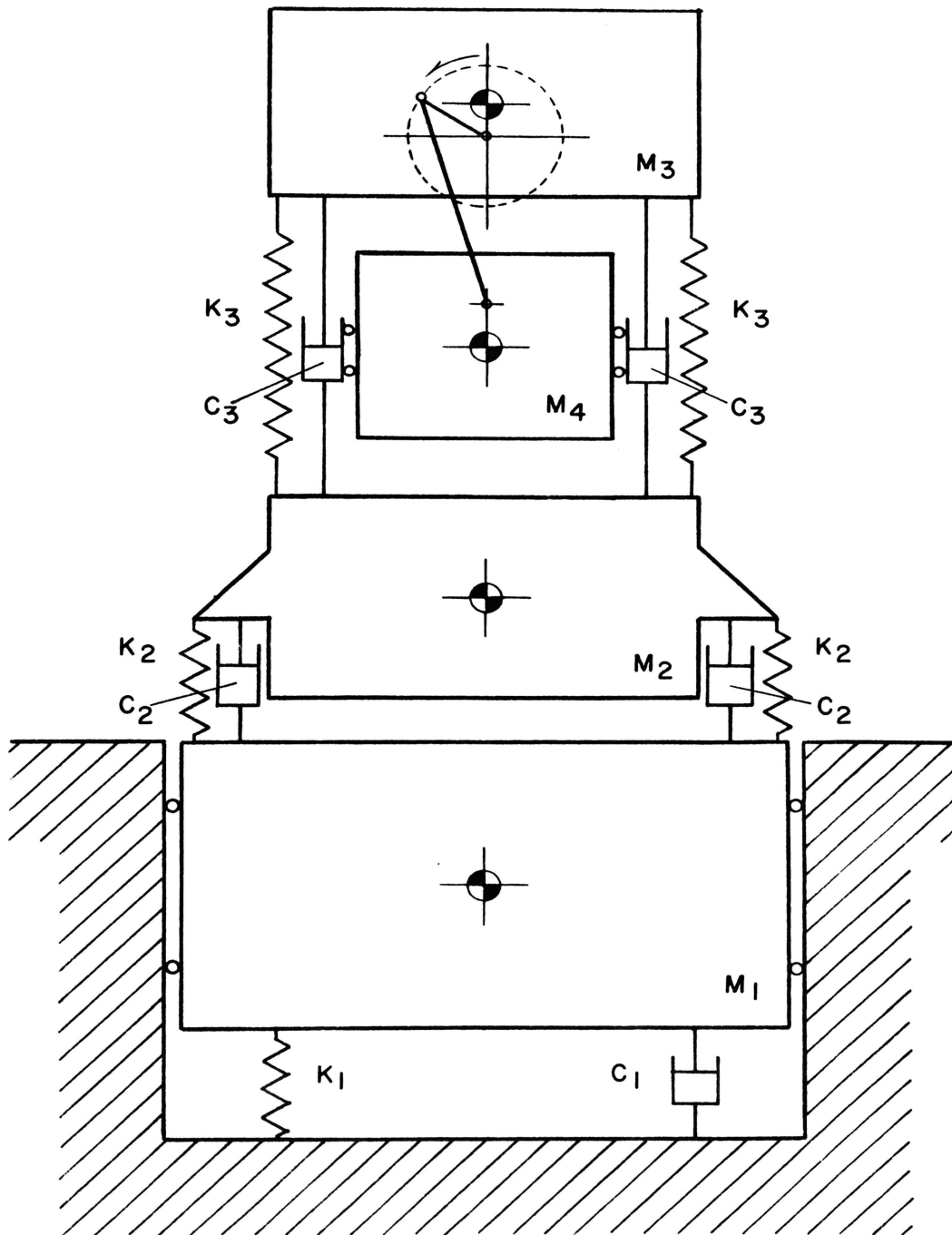


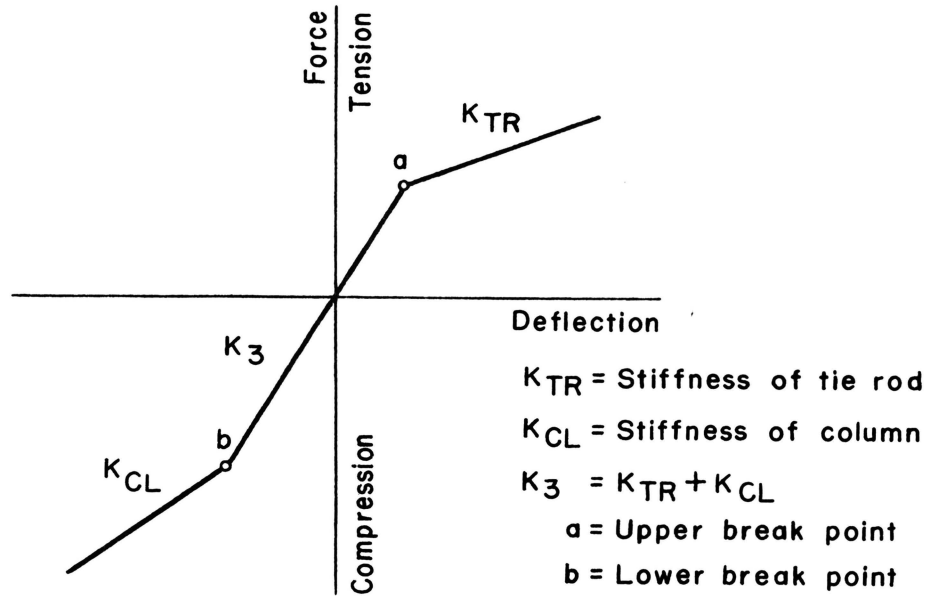
Figure 4. Diagrammatic Sketch Showing Major Elements of the Mathematical Model of the Press

B. Stiffness

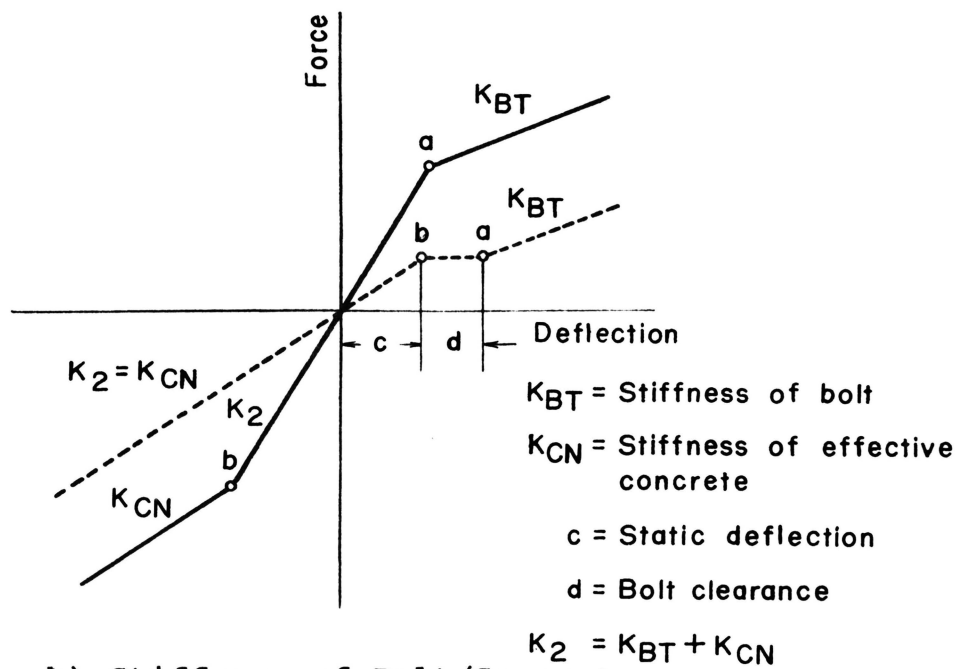
The stiffness between the crown and the bed is calculated on the basis of the total cross-sectional area of the tie rods and the columns. Since the tie rods and the columns are prestressed, this stiffness can have three different values, depending on the deformation, as shown in Figure 5(a). Although stiffness is not a function of the amount of prestress on the tie rods and columns, the two break points (upper and lower) are.

The stiffness between the bed and the foundation is calculated by using the cross-sectional area of the anchor bolts and the effective area of the concrete under the feet of the press, as shown in Figure 5(b). The character of this stiffness is similar to that of the tie rods and columns. When a press is mounted on isolators, the stiffness of the isolators is used as the stiffness between the bed and the foundation.

In most cases, sand is placed beneath the press's foundation. The stiffness of the uniform sand, which is sandwiched between the concrete foundation and the ground, is a function of many parameters, such as size, shape, void ratio, and confining stress. It would be beyond the scope of this paper to discuss soil dynamics in detail, although some of the fundamentals of that area are needed. The stiffness of the sand is expressed by



a) Stiffness of Tie Rod/Column



b) Stiffness of Bolt/Concrete

Figure 5. Force Versus Deflection Curves for Parts of Press

$$K_1 = \frac{G}{1-\nu} \beta \sqrt{A_F}.$$

The shear modulus G is a function of the void ratio of the soil and the confining stress on it, as shown in Figure 6. β is a constant which is a function of the area of the underside of the foundation, as shown in Figure 7 (8).

C. Basic Assumptions

The overall motion of a press during a given operation is complex. Not only is vertical motion prevalent, but rocking, bending, and twisting take place as well. The vertical motion, however, is the primary source of the forces which are transmitted to the foundation and soil, and of the structural vibrations which determine the acoustic radiation level. Therefore, a simplified mathematical model representing the vertical motion has been formulated, based on the following assumptions:

- a) The effects of the horizontal component of forces between the slide and the uprights can be neglected;
- b) The effects of the motor reaction in the drive system can be neglected;
- c) The weight of the connecting rods is negligible;
- d) The rods, as well as the shafts in the driving system, are rigid; and
- e) The axis determined by the centers of gravity of the basic elements passes through the center of

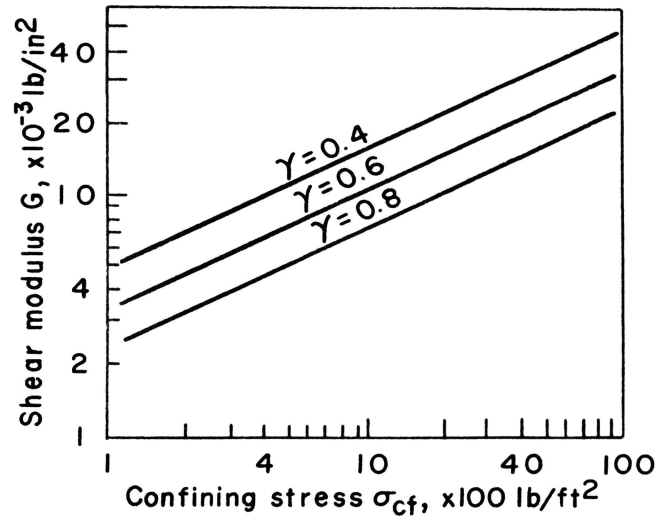


Figure 6. Variation of Shear Modulus of Dry Sand with Void Ratio, γ , and Confining Stress (After Richart (8))

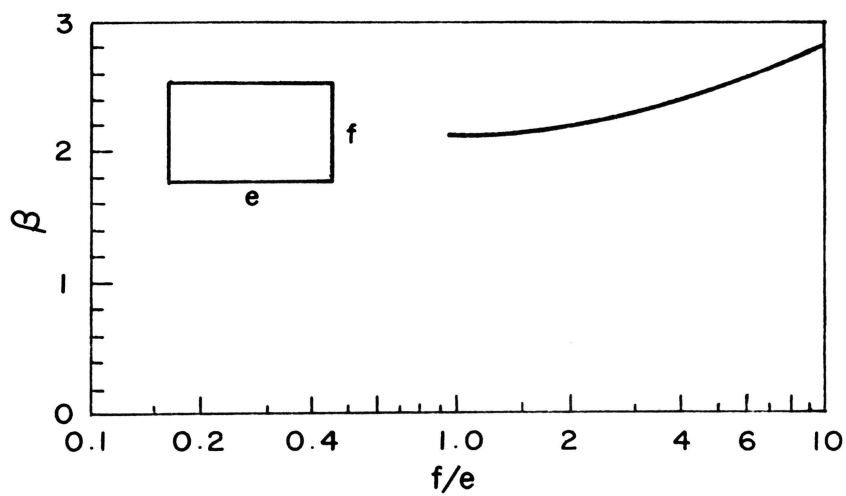


Figure 7. Coefficient β for Rectangular Footings (After Richart (8))

gravity of the total press, and is perpendicular to the floor.

D. Equations of Motion

The governing equations of motion are derived from Newton's Law, and from the free body diagram shown in Figure 8. They are:

$$M_1 \ddot{Y}_1 = 4C_2 (\dot{Y}_2 - \dot{Y}_1) + 4K_2 (Y_2 - Y_1) - C_1 \dot{Y}_1 - K_1 Y_1; \quad (1)$$

$$M_2 \ddot{Y}_2 = 4C_3 (\dot{Y}_3 - \dot{Y}_2) + 4K_3 (Y_3 - Y_2) - 4C_2 (\dot{Y}_2 - \dot{Y}_1) - 4K_2 (Y_2 - Y_1) - F_S; \quad (2)$$

$$M_3 \ddot{Y}_3 = -4C_3 (\dot{Y}_3 - \dot{Y}_2) - 4K_3 (Y_3 - Y_2) + F_B; \text{ and} \quad (3)$$

$$M_4 \ddot{Y}_4 = -F_S + F_B. \quad (4)$$

Combining Eqs. (3) and (4) yields

$$M_3 \ddot{Y}_3 = -4C_3 (\dot{Y}_3 - \dot{Y}_2) - 4K_3 (Y_3 - Y_2) + F_S + M_4 \ddot{Y}_4. \quad (5)$$

Based on Figure 9, the acceleration of the slide, \ddot{Y}_4 , in Eq. (5) can be expressed in terms of θ , $\dot{\theta}$, and \ddot{Y}_3 , where $\dot{\theta}$ is a constant. That figure shows that Y_4 can be written as

$$Y_4 = (R - L) - R \cos \theta + Z - Y_3.$$

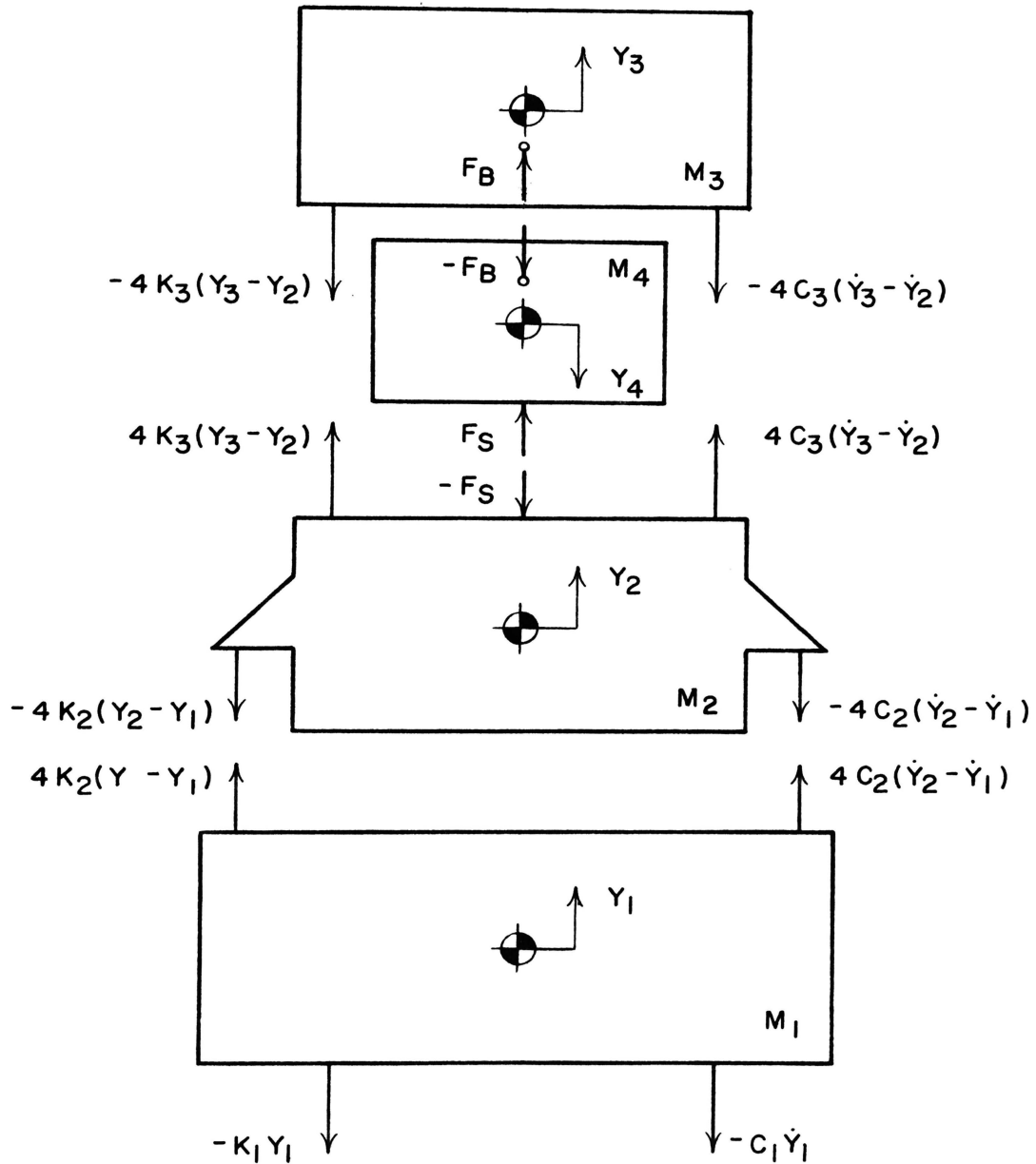


Figure 8. Free Body Diagram of the Major Press Elements

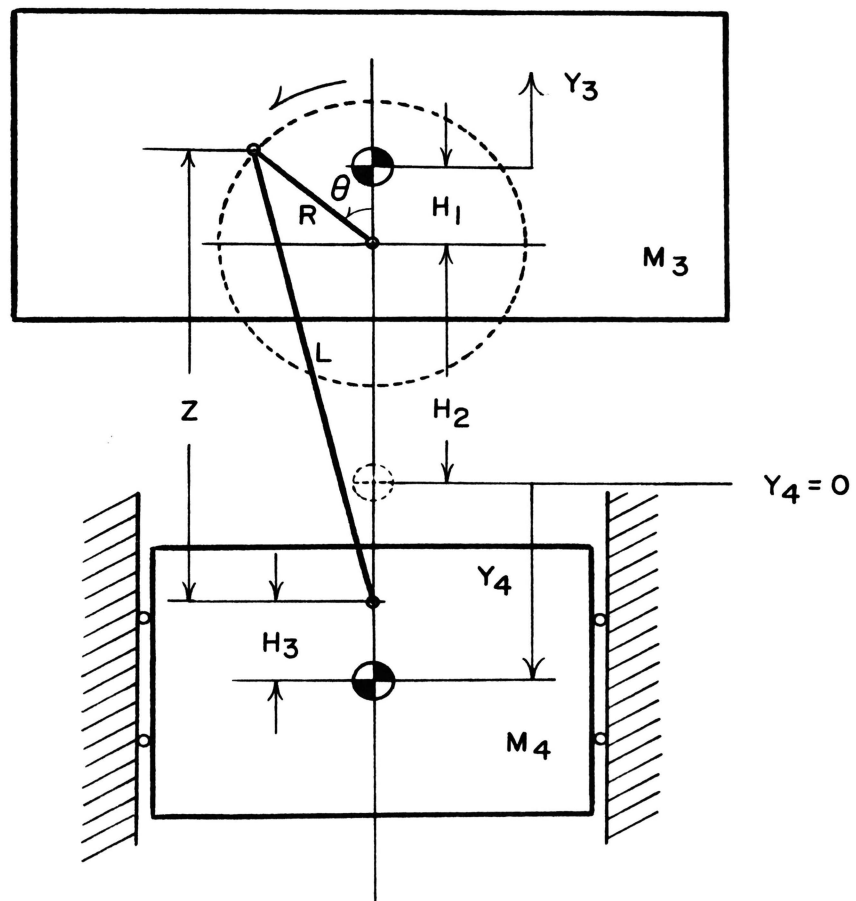


Figure 9. Sketch of the Slide Drive System

Taking the second derivative of that equation yields

$$\ddot{Y}_4 = R \dot{\theta}^2 \cos \theta - \frac{R^2 \dot{\theta}^2}{4 \sqrt{L^2 - \frac{R^2}{2}(1 - \cos 2\theta)}} \left[\frac{R^2 \sin^2 2\theta}{L^2 - \frac{R^2}{2}(1 - \cos 2\theta)} + 4 \cos 2\theta - \ddot{Y}_3 \right]. \quad (6)$$

Thus, Eq. (5) can be expressed in terms of the angular velocity of the crankshaft, which is constant, and \ddot{Y}_3 , rather than in terms of \ddot{Y}_4 . Hence,

$$(M_3 + M_4) \ddot{Y}_3 = -4C_3 (\dot{Y}_3 - \dot{Y}_2) - 4K_3 (Y_3 - Y_2) + F_S + M_4 R$$

$$\left[\dot{\theta}^2 \cos \theta - \frac{R \dot{\theta}^2}{4 \sqrt{L^2 - \frac{R^2}{2}(1 - \cos 2\theta)}} \left\{ \frac{R^2 \sin^2 2\theta}{L^2 - \frac{R^2}{2}(1 - \cos 2\theta)} + 4 \cos 2\theta \right\} \right]. \quad (7)$$

Equations (1), (2), and (7) are the governing equations of the press, and can be rewritten in matrix form as

$$\begin{bmatrix} M_1 & 0 & 0 \\ 0 & M_2 & 0 \\ 0 & 0 & M_3+M_4 \end{bmatrix} \begin{Bmatrix} \ddot{Y}_1 \\ \ddot{Y}_2 \\ \ddot{Y}_3 \end{Bmatrix} + \begin{bmatrix} 4C_2+C_1 & -4C_2 & 0 \\ -4C_2 & 4(C_3+C_2) & -4C_3 \\ 0 & -4C_3 & 4C_3 \end{bmatrix} \begin{Bmatrix} \dot{Y}_1 \\ \dot{Y}_2 \\ \dot{Y}_3 \end{Bmatrix} \\
+ \begin{bmatrix} 4K_2+K_1 & -4K_2 & 0 \\ -4K_2 & 4(K_3+K_2) & -4K_3 \\ 0 & -4K_3 & 4K_3 \end{bmatrix} \begin{Bmatrix} Y_1 \\ Y_2 \\ Y_3 \end{Bmatrix} = \begin{Bmatrix} 0 \\ -F_S(t) \\ F_S(t)+M_4R\dot{\theta}^2 \end{Bmatrix}, \quad (8)$$

where

$$\dot{\theta}^2 = \dot{\theta}^2 \cos \theta - \frac{R \dot{\theta}^2}{4 \sqrt{L^2 - \frac{R^2}{2}(1 - \cos 2\theta)}} \left[\frac{R^2 \sin^2 2\theta}{L^2 - \frac{R^2}{2}(1 - \cos 2\theta)} + 4 \cos 2\theta \right]. \quad (9)$$

E. Computer Simulation

Numerical solutions for this system of nonlinear differential equations are obtained with the IBM Subroutine RKGS (9) which uses the Runge-Kutta method. This method is based on a fourth-order integration procedure which is stable and self-starting. The main program consists of five subroutines, namely, EIGEN, RKGS, FCT, OUTP, and PLT.

Subroutine EIGEN (9) is used to compute the eigenvalues and eigenvectors from which the natural frequencies and mode

shapes of the system can be evaluated assuming small deflections and linear theory. Subroutine RKGS, which has two external subroutines, FCT and OUTF, is used to obtain an approximate solution of a system of first-order ordinary equations with given initial values. FCT and OUTF are for input and output, respectively. Subroutine PLT is for plotting any output.

The initial values for the solution of the differential equations represent those conditions present at the end of the fourth cycle of the loading. They are obtained by running the main program, considering only the inertial loading. By performing calculations, it was learned that completion of four cycles sufficiently reduces the transient to give a steady state solution. The solution of the differential equations is obtained at the fifth cycle of the loading, including the stamping force, by using the initial conditions. These steps are outlined in the flow chart which is shown in Figure 10.

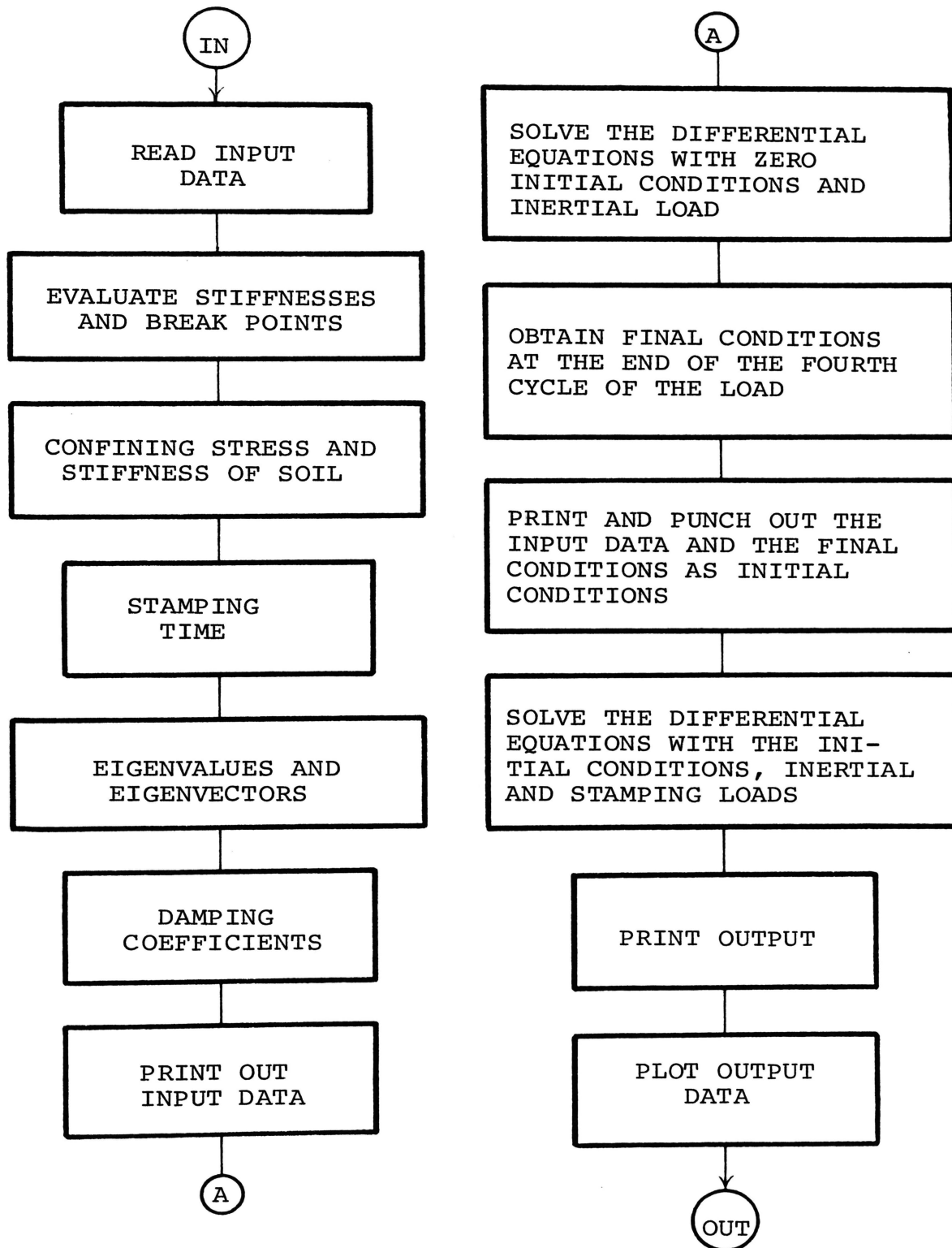


Figure 10. Flow Chart Showing Major Steps in Performing Computer Calculations

IV. EXPERIMENTAL TESTS

Field experiments have been carried out utilizing a 60 ton, tie rod, straight-sided press (Bliss, Serial No. H-48291) at the Schwitzer Division of the Wallace-Murray Corporation in Rolla, Missouri. The total press weighs approximately 14,000 lb. with feed. The unit has two connecting rods, a three-inch stroke, and 200 percent pre-stressed tie rods. The press is shown in Figure 11. More detailed specifications are given in Appendix A. To obtain the stamping force during press operation, two strain gauges (ED-DY-250BG-350, Micro-Measurements) forming a full bridge are mounted on each connecting rod. The press is isolated, and rests on a six-inch reinforced concrete floor.

A. Tests

Accelerations of the crown and bed, velocities of the floor, and strains of the connecting rods have been measured. All the data have been recorded with an FM tape recorder (Tandberg, Series 100) through amplifiers. After recording the data, known signals were inserted into the tape recorder using a vibration exciter (MB, Electronics, Model C25HHA, Serial No. 526) in order to calibrate the data. Following the calibration, the data were sampled on the NOVA terminal and then transmitted to the IBM-360 computer and plotted. The general scheme is shown in Figures 12 and 13.



Figure 11. Photograph of Press on Which Field Measurements were Taken



Figure 12. Photograph of Instrumentation
Used in the Field

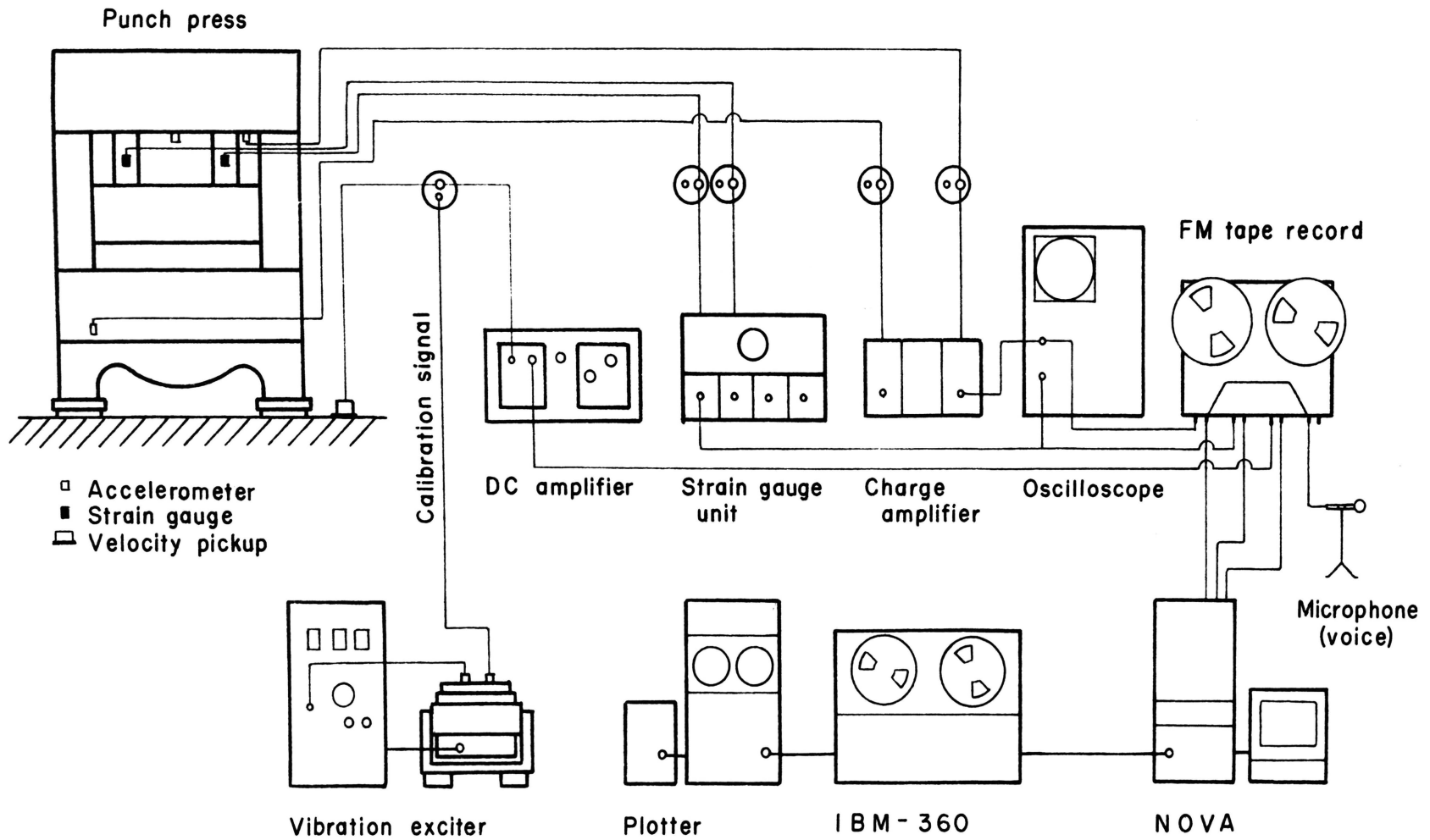


Figure 13. Diagrammatic Arrangement of Instrumentation and Computers

B. Results

The purpose of the experimental test program is to support the validity of the mathematical model by comparing the results of the tests with computer simulations using the same speed and stamping loads. Stamping forces are found from the force histories of the connecting rods, $F_{CR}(t)$, with the relation

$$F_S(t) = F_{CR}(t) \cos \theta(t) - M_4 \ddot{Y}_4(t).$$

$F_{CR}(t)$ is evaluated using the strain histories of the connecting rods, their elastic modulus, and their area.

The force pulse during stamping is of right triangular shape. The specific shape depends on the hardness and the thickness of the material processed, the break clearance of the die set, and the speed of the driving system. A typical recorded stamping pulse is shown in Figure 14. This pulse results from the two blanking operations which occur almost simultaneously. The punching of four small holes causes the small downward peak on the left side of the pulse. The main blanking operation follows, which results in the large, center downward peak, the magnitude of which is 68,000 lb. This force is 57 percent of the rated capacity of the press. The small upward peak on the right side of the pulse reflects the tension of the connecting rod just after the stamping operation.

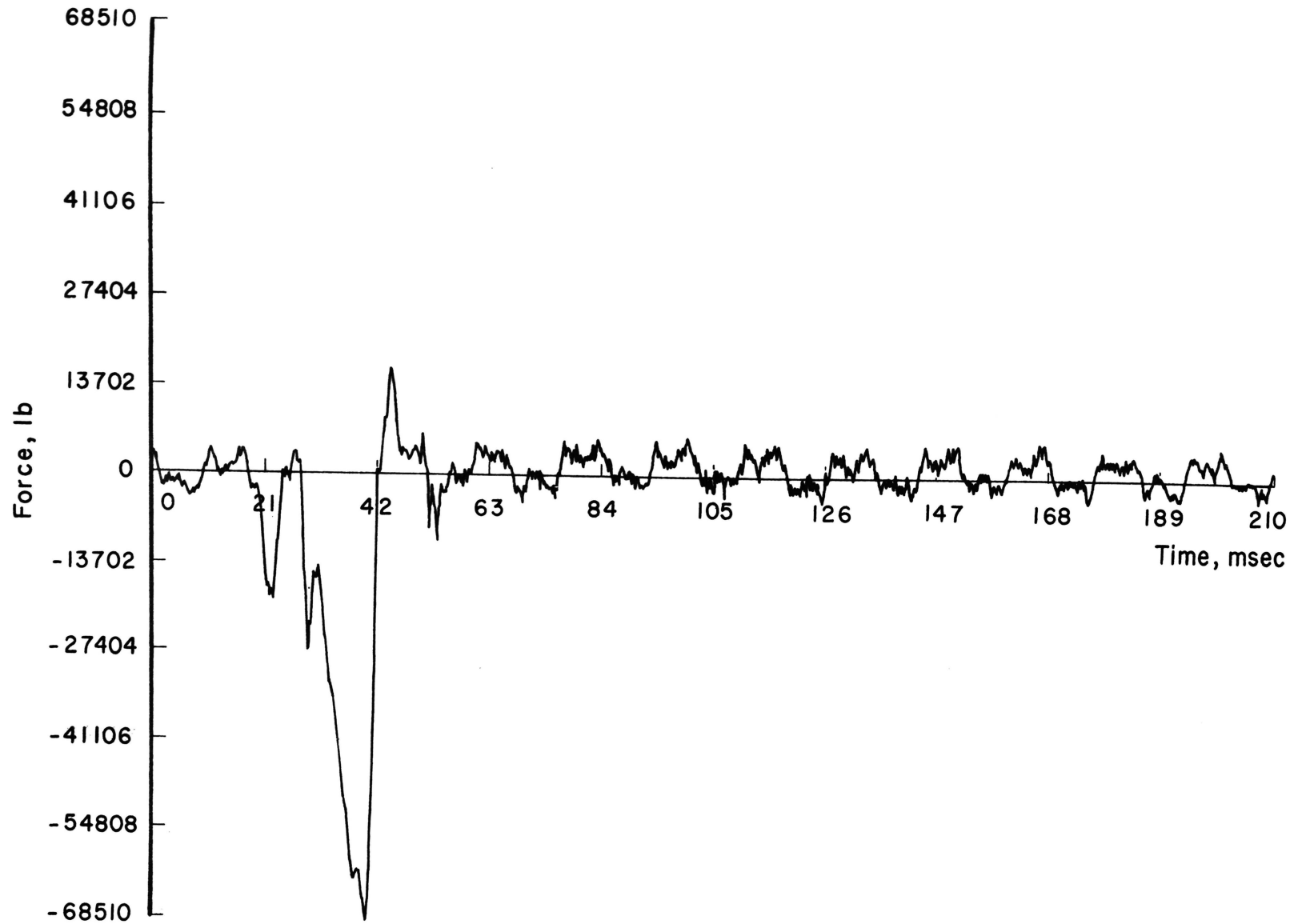


Figure 14. Recorded Stamping Pulse

Four sets of field measurements have been conducted with two different sets of isolators, having frequencies of 19.4 and 9.9 Hz. The first two sets of measurements were recorded on tape and plotted by the computer. After the first set of measurements were made, the 19.4 Hz isolators were replaced by ones having a natural frequency of 9.9 Hz in order to compare the performances of the two sets of isolators. The maximum levels of acceleration resulting from the four sets of measurements, and their approximate locations, are shown in Figure 15. It is noted that the acceleration levels from the first measurement are approximately half those from the other three measurements. Later, it was learned that an ungrounded charge amplifier used during the first measurement was responsible for that inconsistent data.

The acceleration magnitudes are higher at the middle of the crown and bed than they are near the side frames. This indicates bending effects in the crown and bed frames. The acceleration of the crown near the side frame during the second measurement is shown in Figure 16. The major group of oscillations consists of two parts, as will be shown more clearly in the computer simulation. The maximum value, 9.0, occurs just at the end of the stamping operation. The decay of the acceleration curve allows calculation of the press's damping ratio; for this unit the value is determined to be $\zeta = 0.007$.

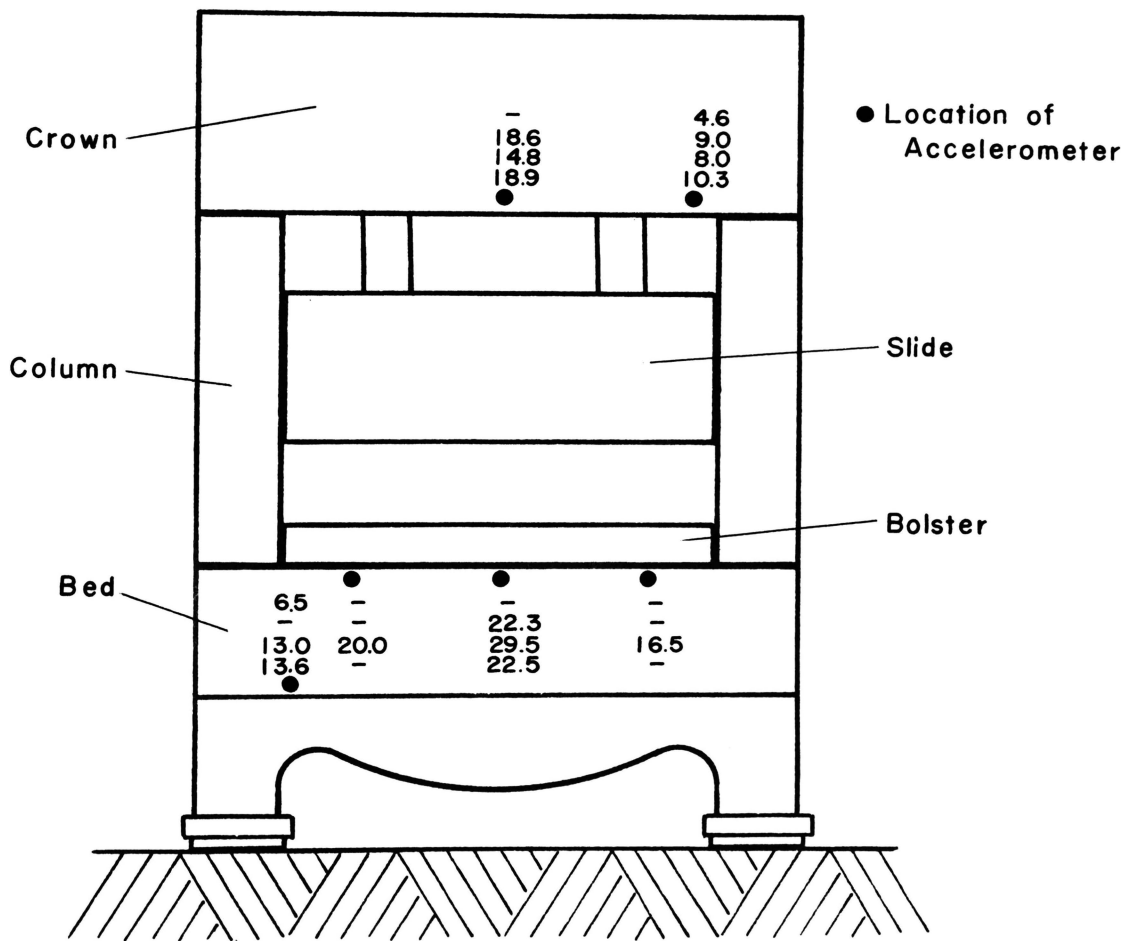


Figure 15. Schematic Diagram Showing Maximum Accelerations Recorded at Various Locations on the Press

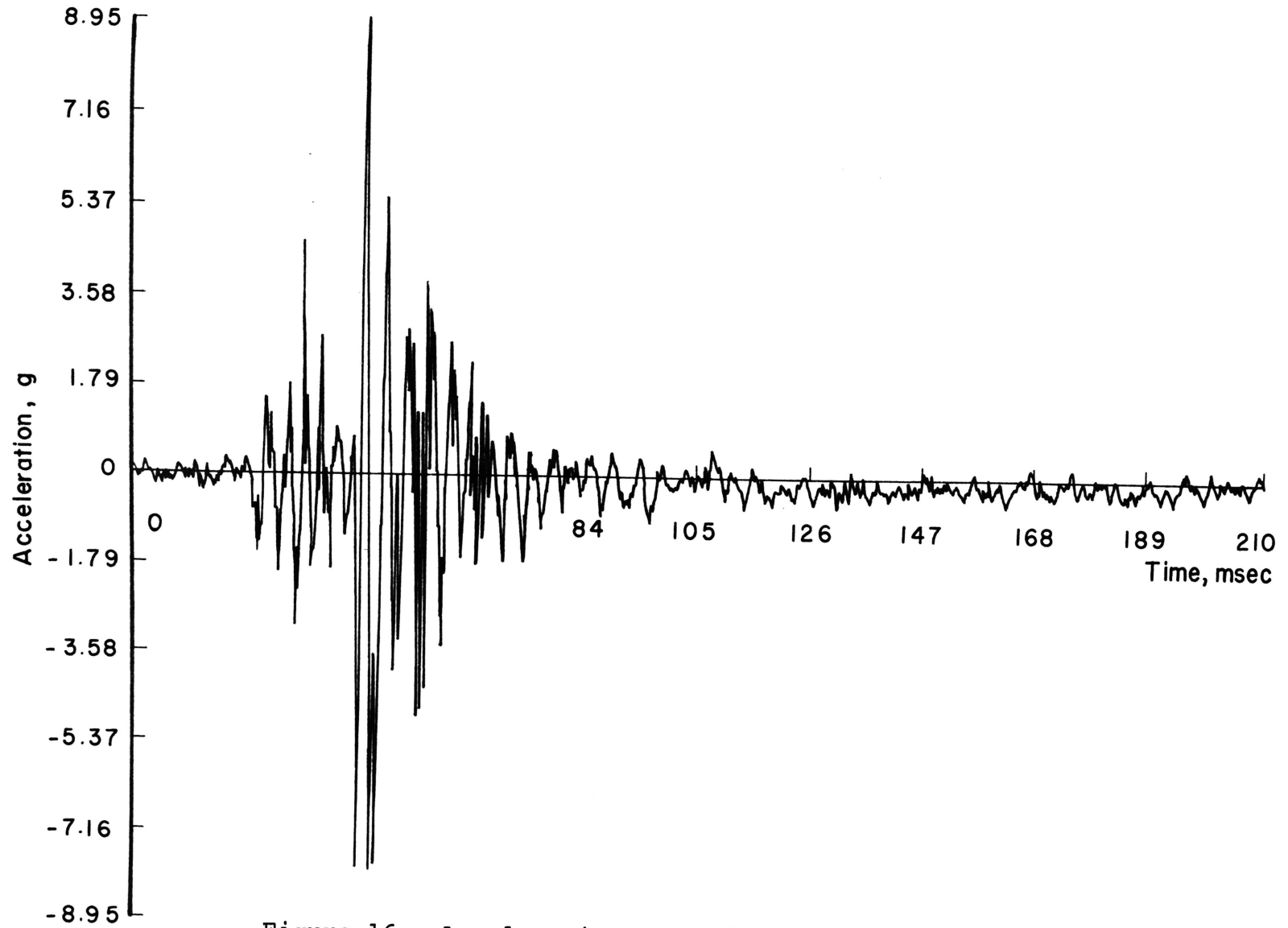


Figure 16. Acceleration Recording from the Crown

The acceleration of the bed near the side frame during the second measurement set was accidentally omitted during the recording. However, the maximum value at the location was measured as 13.0 g and 13.6 g during the third and fourth measurements, respectively. A higher level of acceleration and frequency occurs at the bed, since it has less mass than the crown. The location of the lower die and bolster plate at the bed also contributes to the occurrence of higher frequency oscillations there.

The acceleration of the bed near the side frame and its frequency spectrum are shown in Figures 17 and 18, respectively. From Figure 17, the dominant frequency of the major group of oscillations has been calculated to be in the neighborhood of 470 Hz, corresponding to the 471 Hz value which is one of the four major frequencies in the spectrum shown in Figure 18. This spectrum is obtained using the fast Fourier transform, a subprogram built into the NOVA computer.

The accelerations of the crown and the bed generated by the computer simulation are 8.0 g and 13.5 g, respectively, at 421 Hz. They are shown in Figures 19 and 20, respectively. The frequency, 421 Hz, is the highest of the system's three natural frequencies which are evaluated with the subroutine EIGEN, and it corresponds to the mode in which the crown and bed move in opposition to each other.

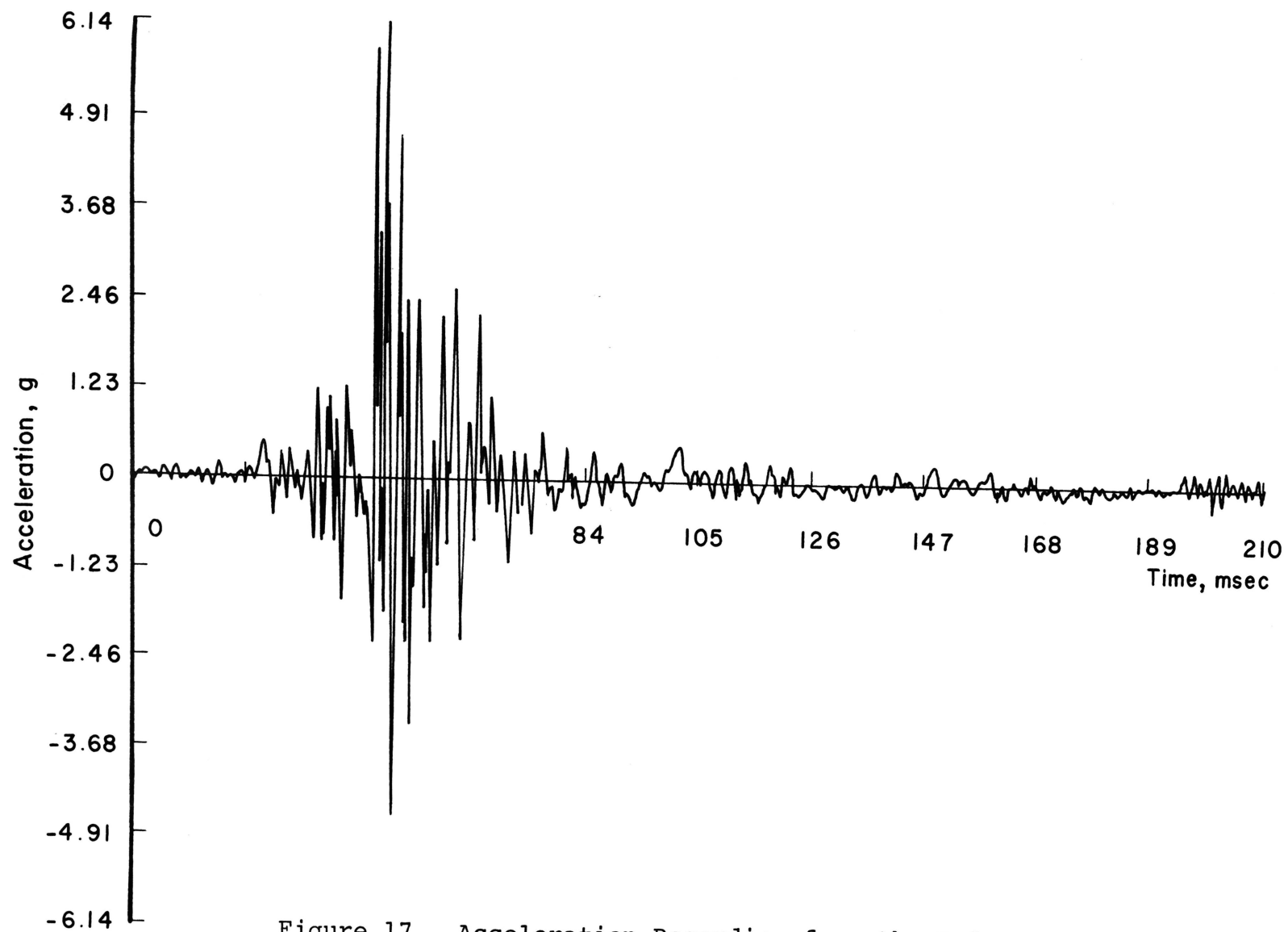


Figure 17. Acceleration Recording from the Bed

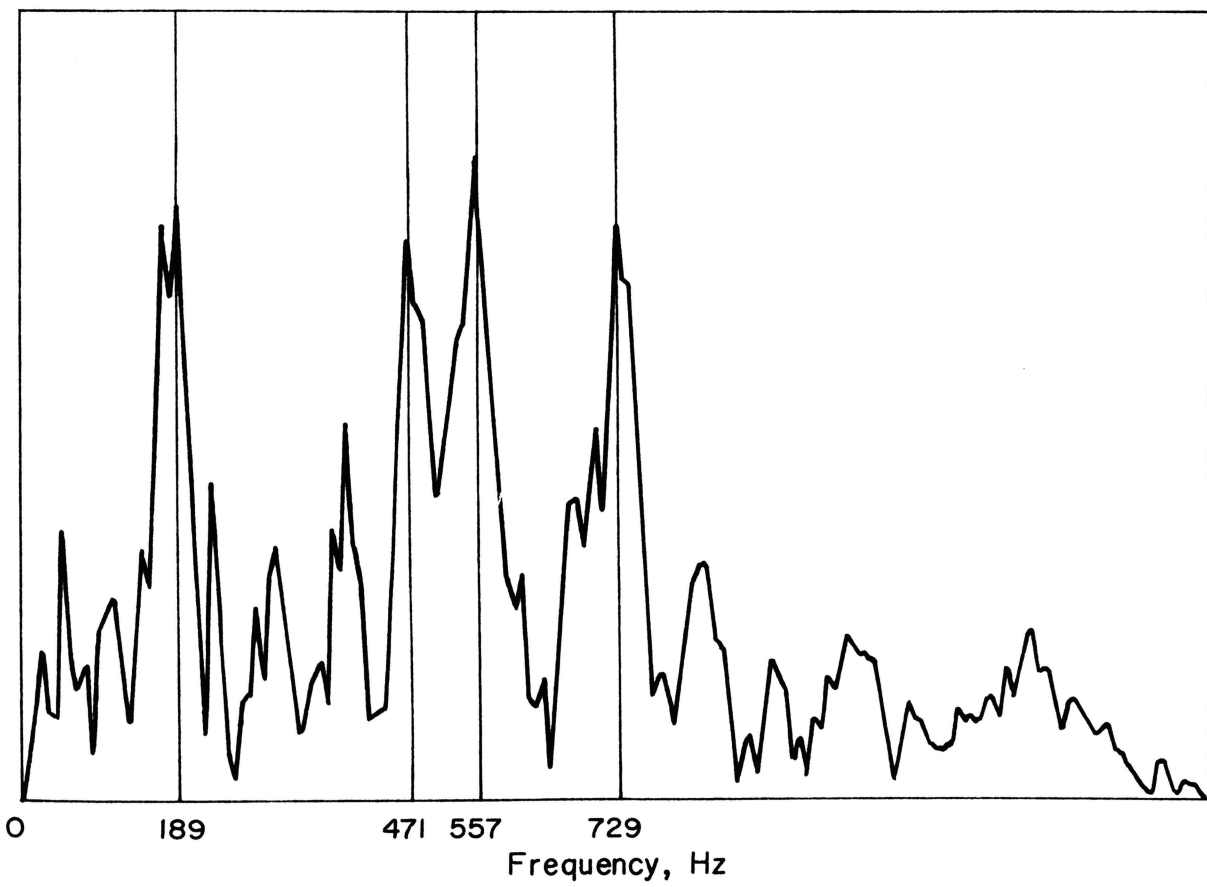


Figure 18. Frequency Spectrum of Signal Shown in Figure 17

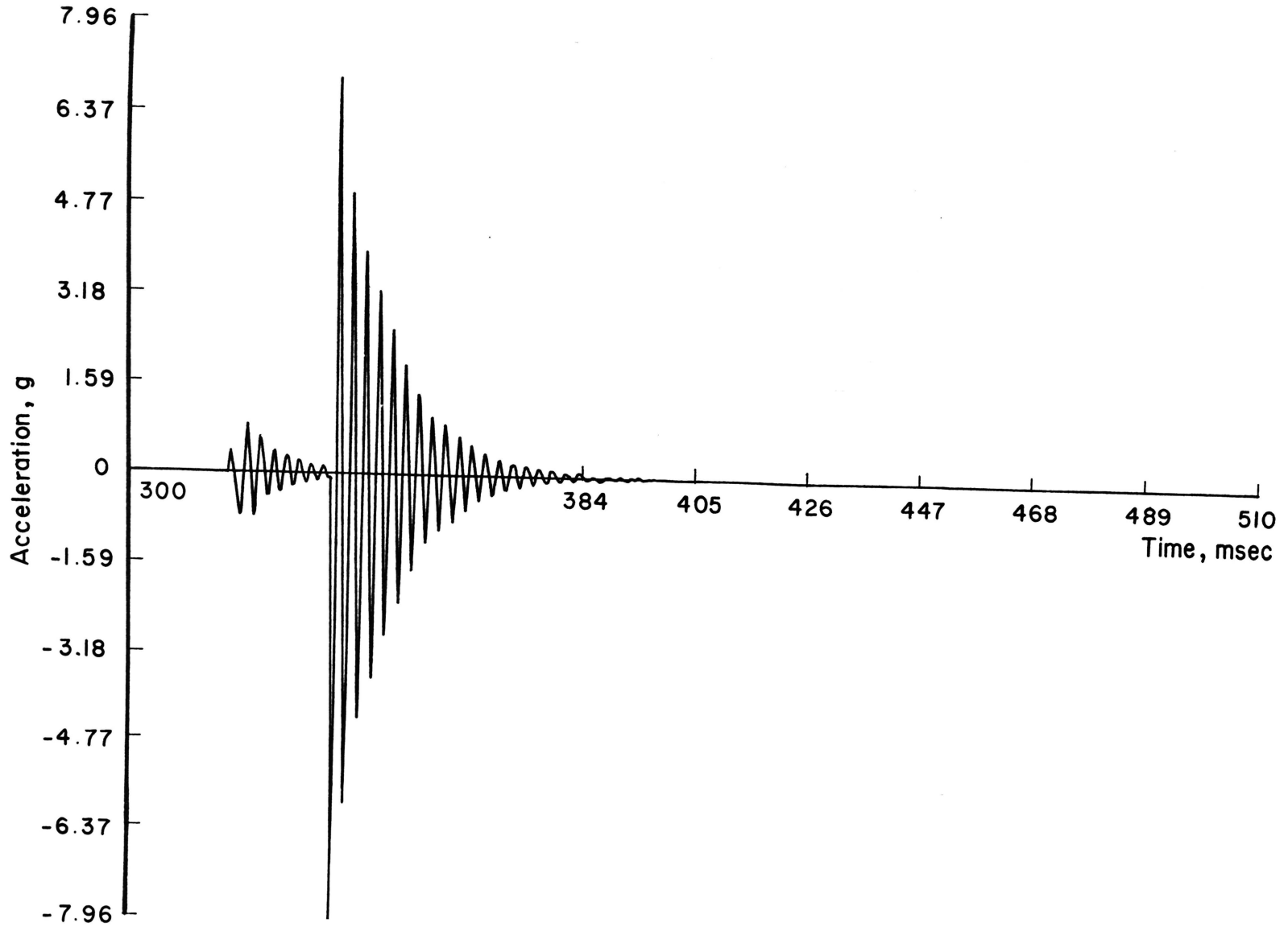


Figure 19. Computer Simulation Showing Crown Acceleration

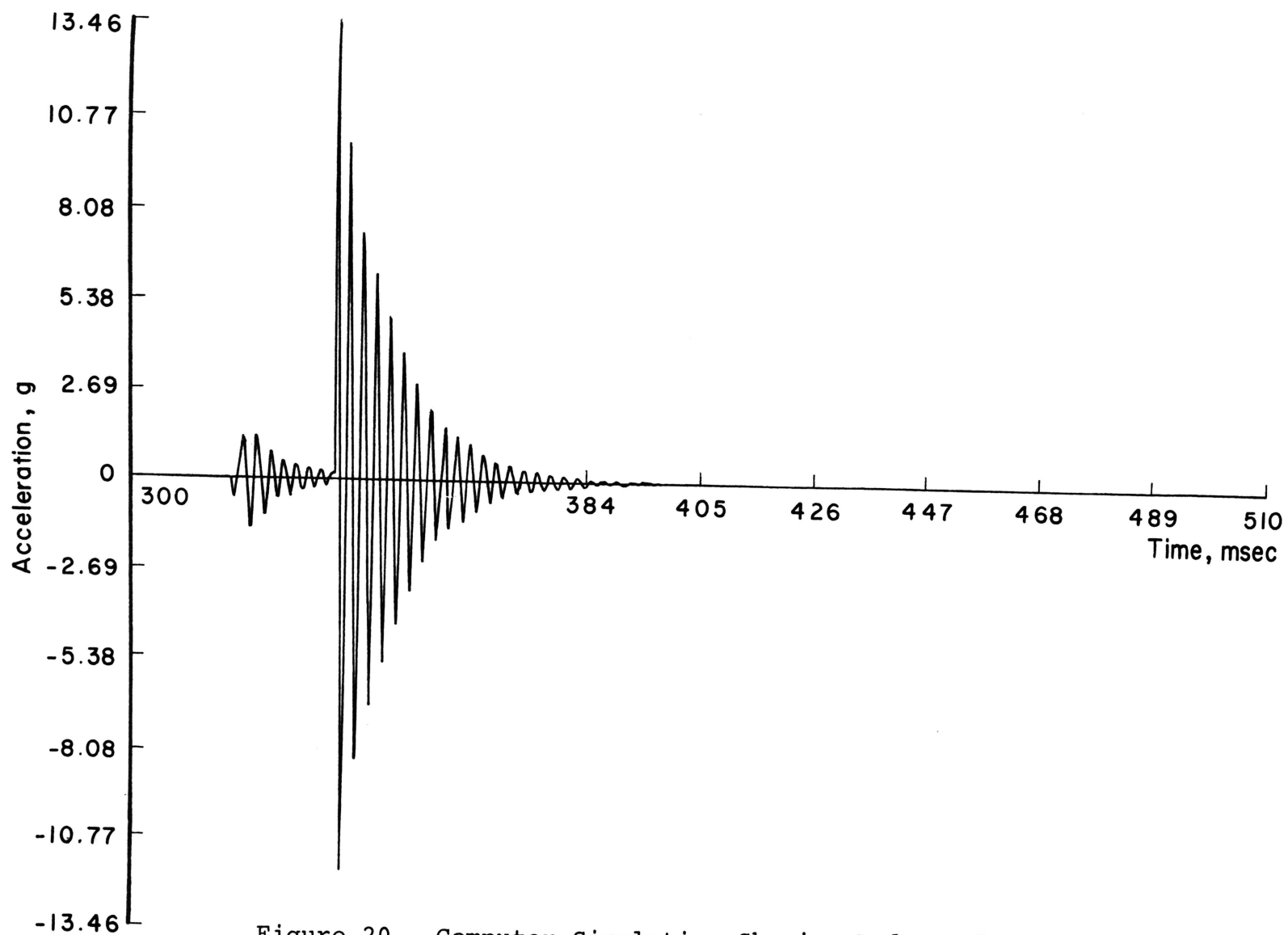


Figure 20. Computer Simulation Showing Bed Acceleration

This frequency is approximately eleven percent less than the 471 Hz value in the spectrum of the measured signal.

Two groups of oscillations are shown in the figures, resulting from the two blanking operations which occur almost simultaneously. This type of response was also evident in the acceleration of the crown shown in Figure 16.

The frequency of the floor velocity is observed to be approximately 20 Hz, as determined from Figure 21. The critical damping ratio of the soil under the floor is determined to be 0.009 by a calculation based on the logarithmic decrement. The maximum velocity is 0.12 in/sec at the end of the stamping operation. Noise from the adjacent presses is observed in the signal from the velocity pickup, as well as the 471 Hz oscillation of the crown and bed near the maximum amplitude.

The latter is more clearly shown in the computer simulation of the foundation velocity shown in Figure 22. In that simulation, 0.6 times the press's mass was used as the foundation mass, resulting in a response frequency of 32 Hz with 0.04 in/sec as the maximum velocity. Since the press is isolated and rests on a six-inch reinforced concrete floor, rather than on a massive concrete foundation, the data relating to the floor vibration generated by the computer simulation were not expected to correlate especially well with the experimental results.

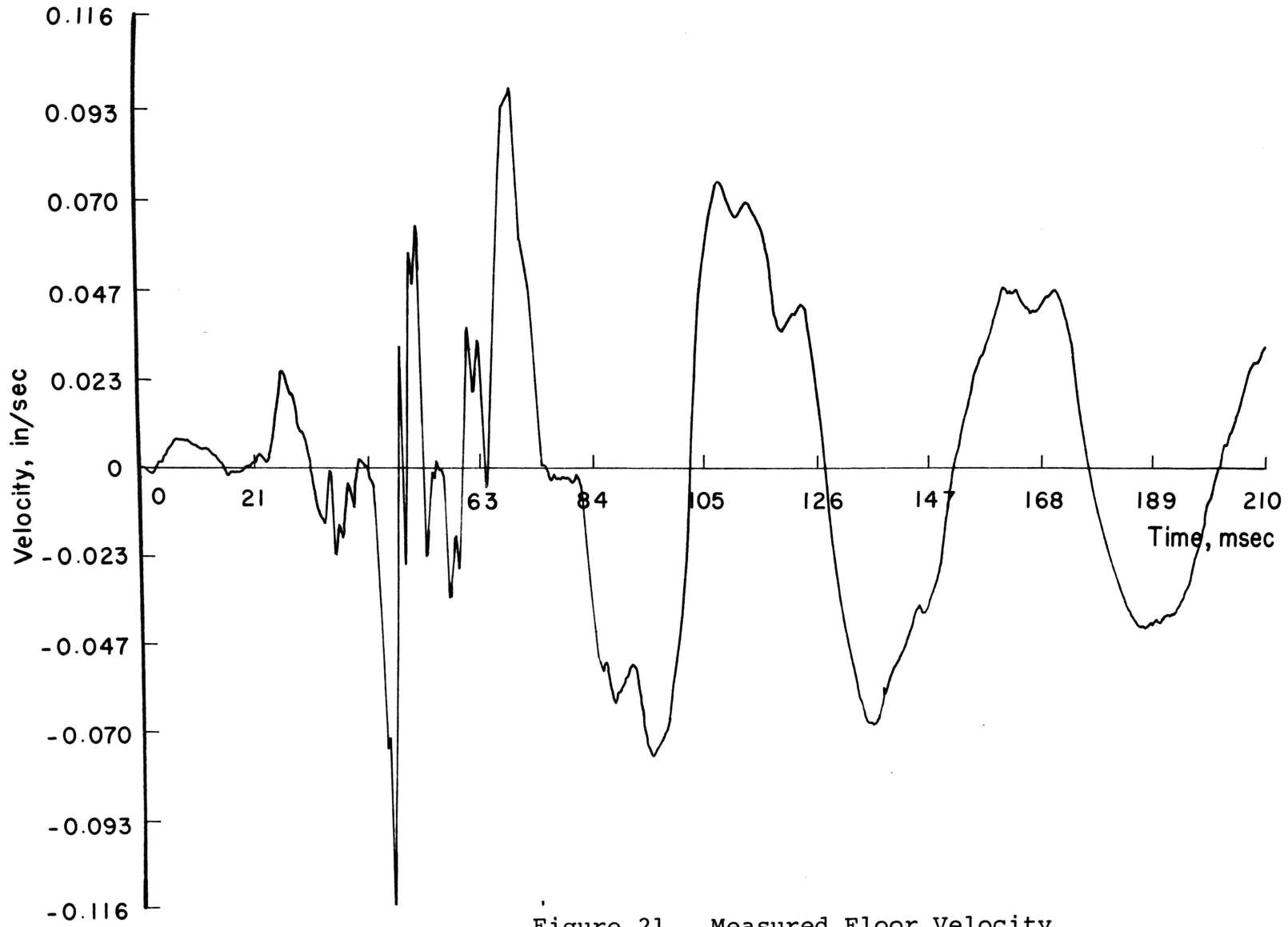


Figure 21. Measured Floor Velocity

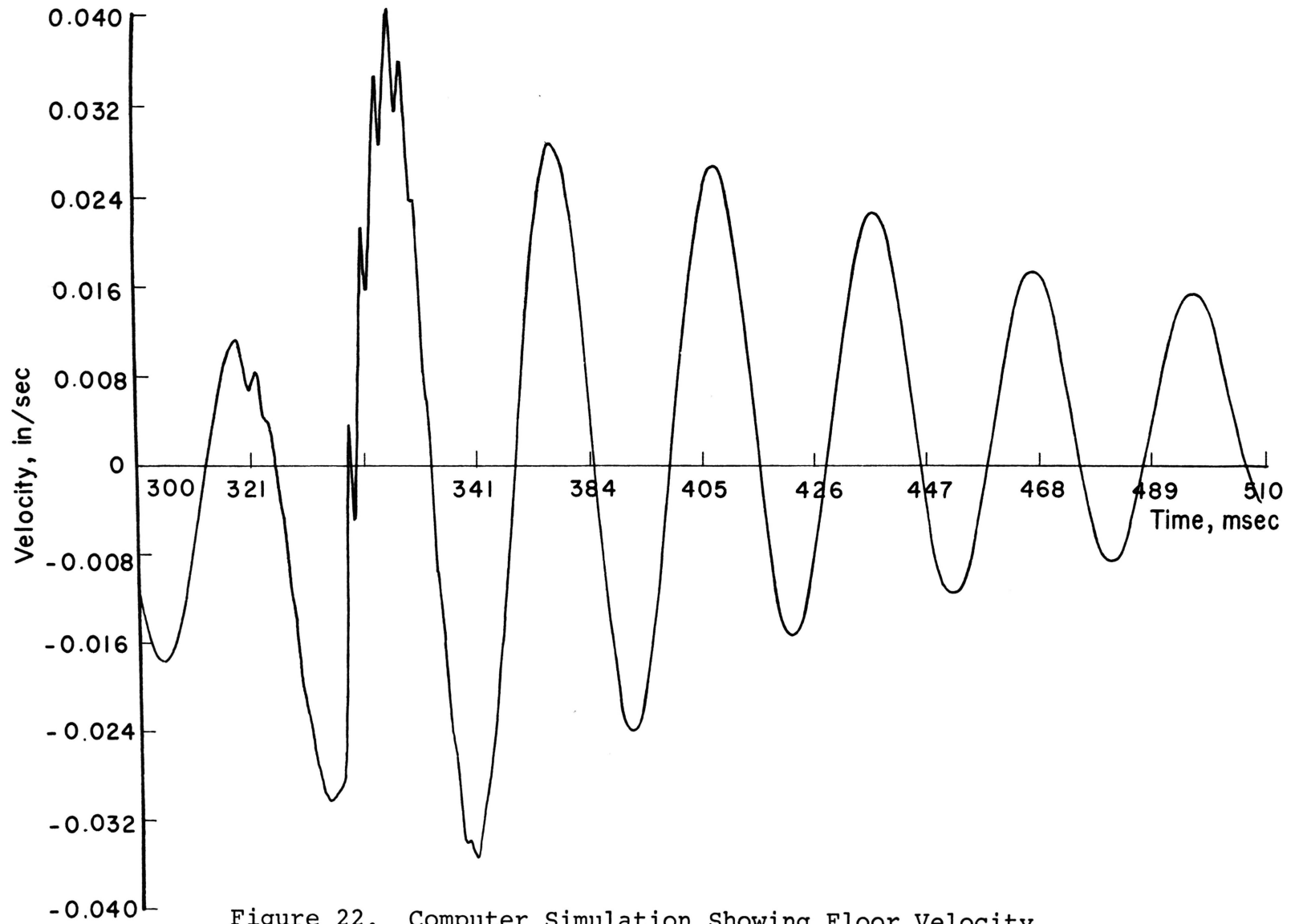


Figure 22. Computer Simulation Showing Floor Velocity

It is, therefore, interesting to note that simulation results for the accelerations of the crown and bed are 8.0 g and 13.5 g, respectively, while the experimental results show average values of 9.1 g and 13.3 g. Thus, the difference between the experimental data and the values generated by the computer simulation at the crown is 1.1 g, and at the bed is only 0.2 g. These values represent variances of about twelve percent of the experimental value at the crown, and about two percent of the experimental value at the bed.

V. EXTENDED SIMULATION STUDIES

A 600-ton tie rod type press was chosen as the subject of a further computer study to show: a) the effects of varying the foundation mass of a bolted press; b) the effects of loosened anchor bolts; and c) the effects of varying the foundation mass of a press resting on isolators. The entire press weighs approximately 172,000 lb with feed, has 175 percent prestressed tie rods, and has four connecting rods which drive the slide through a 10-inch stroke at a speed of 60 strokes per minute. More detailed specifications are given in Appendix B.

This is not only the most common type of press (a tie rod straight-sided frame), but is also a high capacity press which is usually used with a massive foundation block. Thus, this particular press is ideal for studying a mathematical model simulation which includes the foundation mass.

A right triangular shaped loading pulse with a peak value of 1,200,000 lb was used as the stamping force. This magnitude corresponds to 100 percent of the press's capacity.

A. The Effects of Varying the Foundation Mass of a Bolted Press

The press is bolted down by four anchor bolts two inches in diameter and 27 inches long. These bolts were

prestressed to half of the yield stress when the press was mounted in place.

For one cycle of the press's operation, the displacements and accelerations of the crown and bed and the velocity of the foundation are shown in Figures 23, 24, 25, 26, and 27. The speed of the inertial loading, 60 strokes per minute, generates a press frequency of one Hz. This is illustrated in Figures 23 and 24, showing its overall resemblance to a cosine curve (see also Figures 36 and 37). The stamping operation, which has a duration of 0.0076 sec., starts at 0.4154 sec.

The frequencies of the crown and the bed just after the stamping operation are calculated, from Figures 23 and 24, to be 84 Hz and 197 Hz, respectively. The higher frequency at the bed results from the fact that the bed has less mass than the crown and is coupled to the foundation with a stiffness of the same order as the stiffness of the tie rods and columns.

The force transmitted to the foundation is of two kinds: the static force, determined by the weight of the press, and the dynamic force, determined by the inertial and stamping loads. The latter includes a tensile force in this case. The transmitted force versus time is shown in Figure 28. The maximum dynamic load which is compressive is calculated to be 1.34×10^6 lb, which is 7.8 times the static weight of the press. The curves below the time

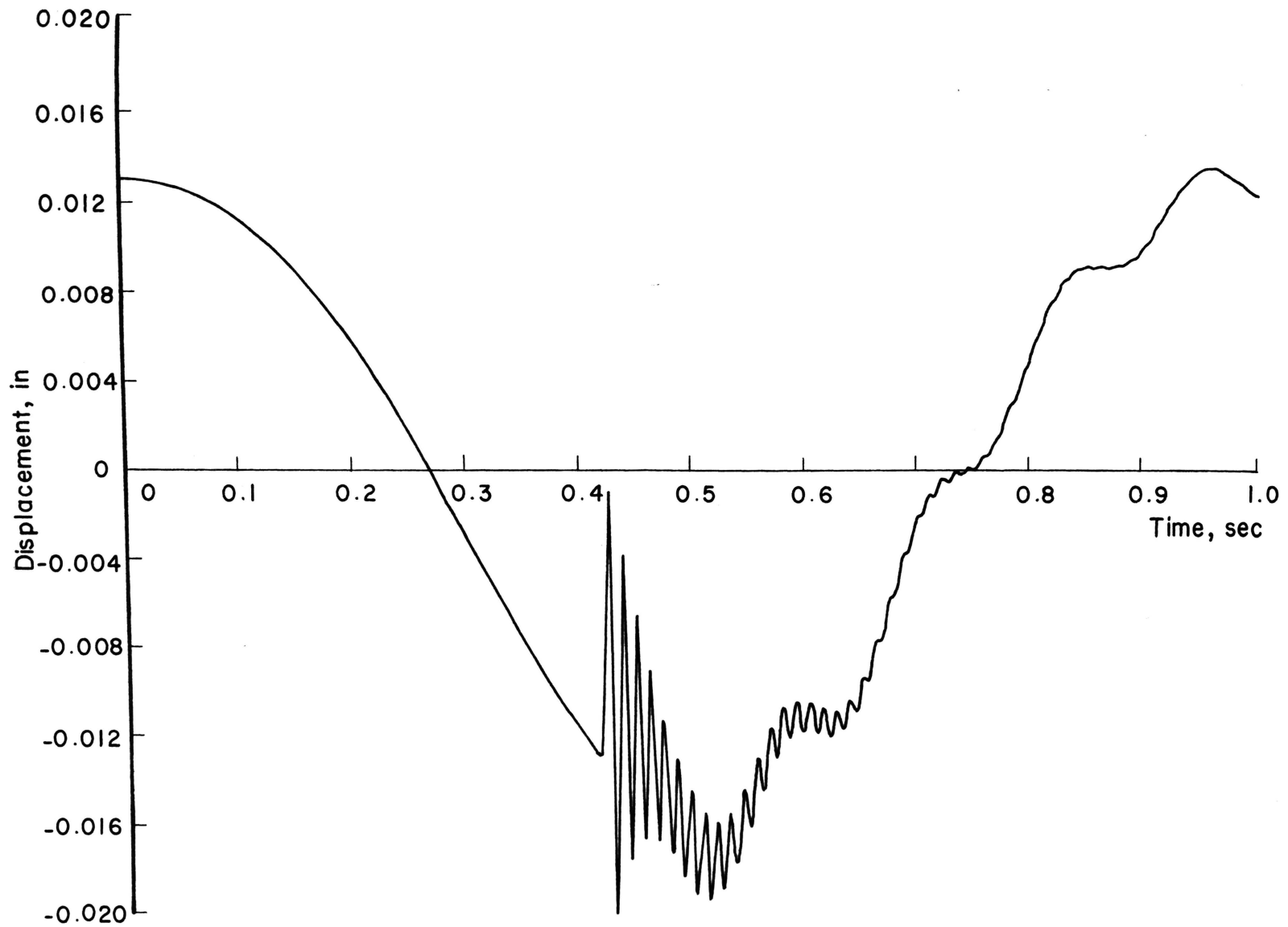


Figure 23. Simulation of a Bolted Press Showing Crown Displacement.

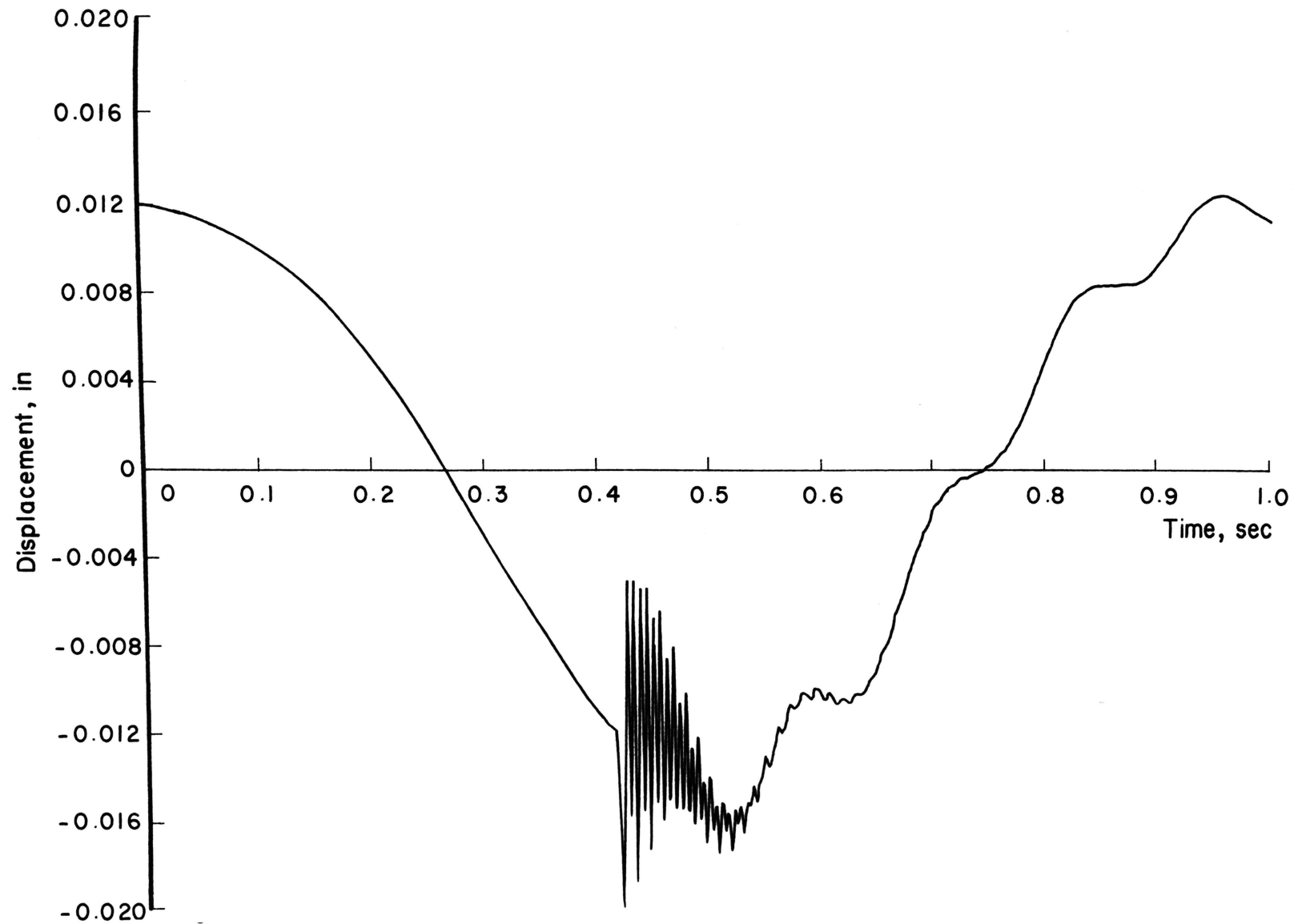


Figure 24. Simulation of a Bolted Press Showing Bed Displacement

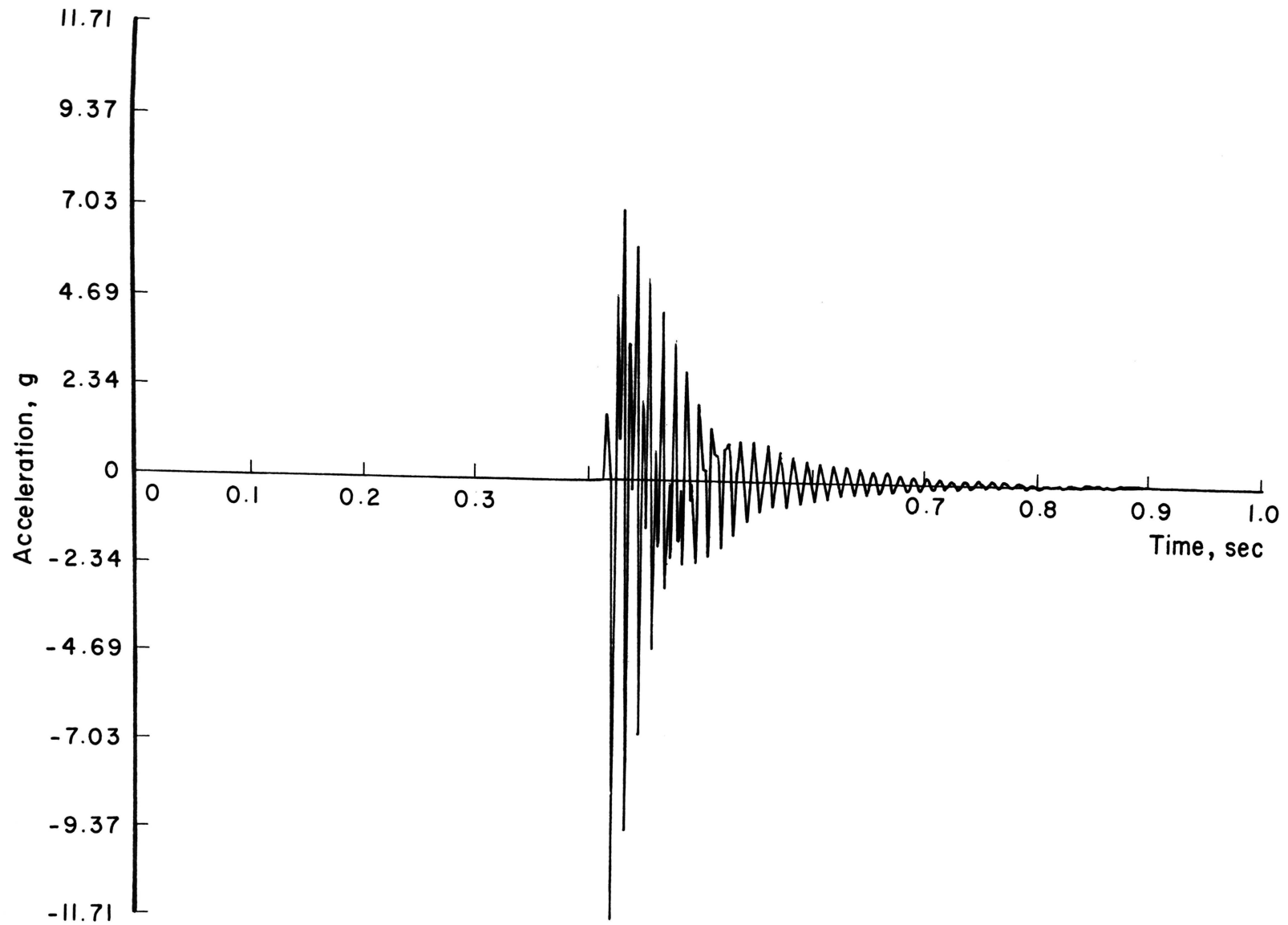


Figure 25. Simulation of a Bolted Press Showing Crown Acceleration

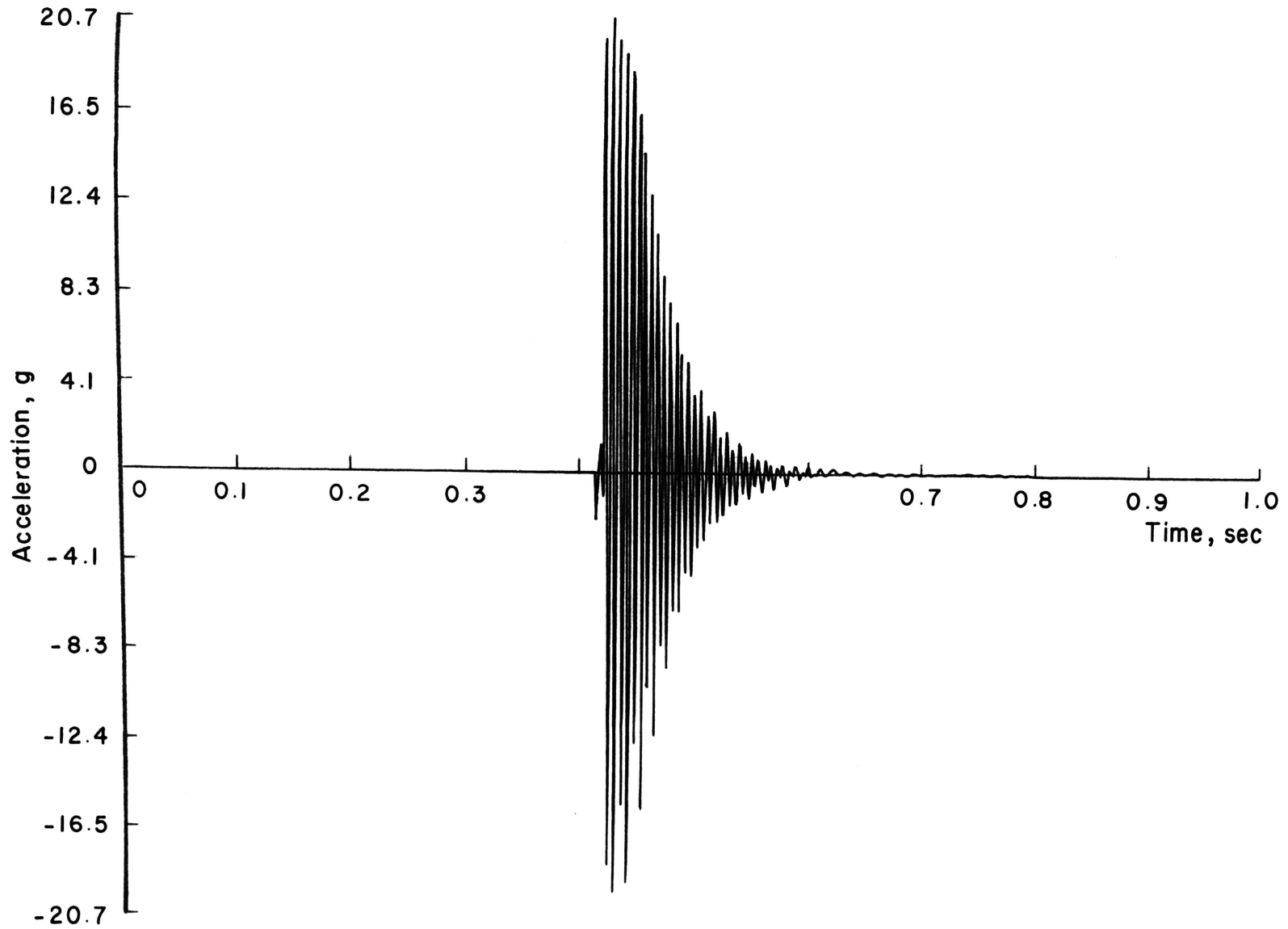


Figure 26. Simulation of a Bolted Press Showing Bed Acceleration

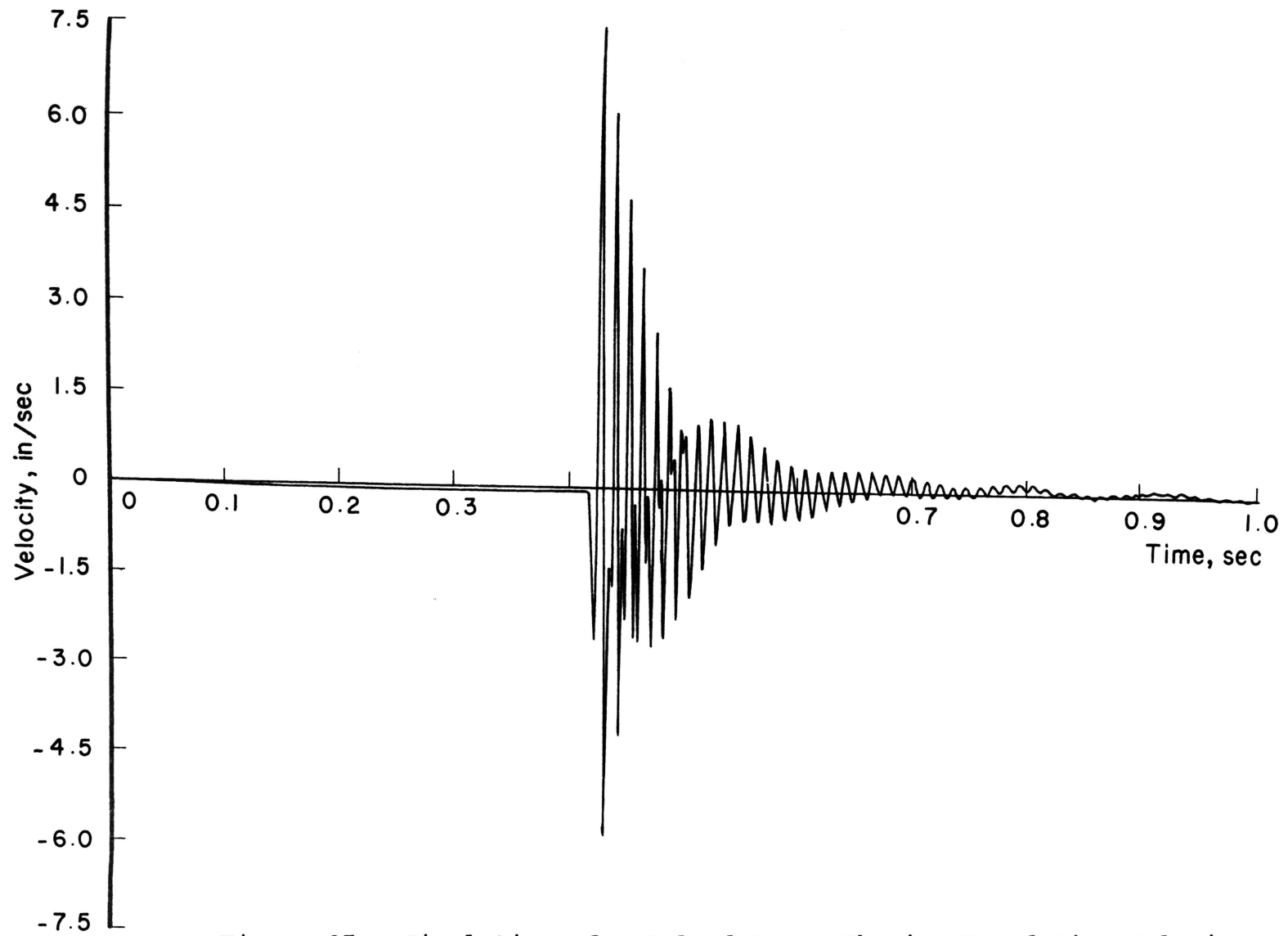


Figure 27. Simulation of a Bolted Press Showing Foundation Velocity

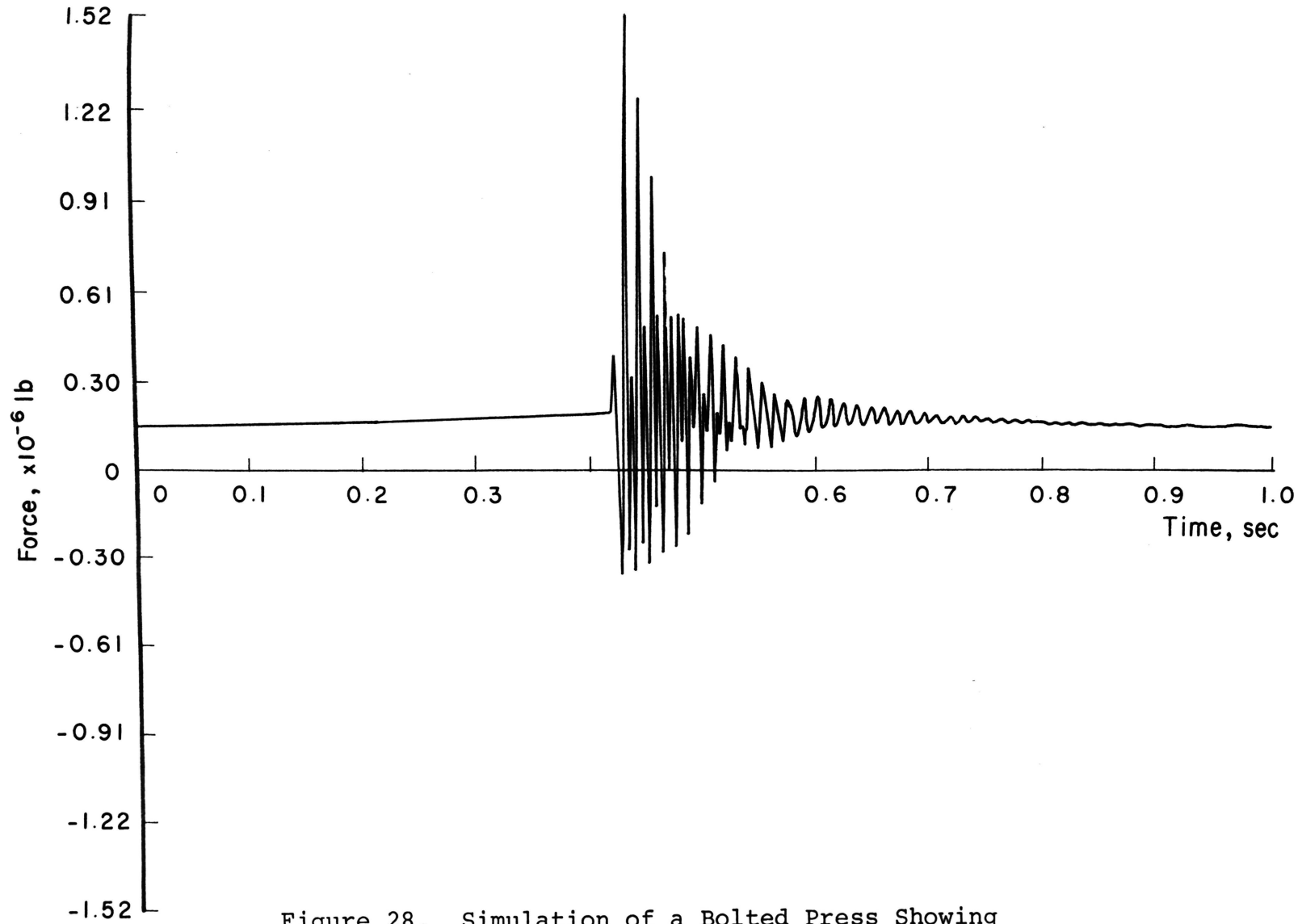


Figure 28. Simulation of a Bolted Press Showing Force Transmitted to the Foundation

axis in the figure represent tensile forces which result from the positive relative displacement between the bed and the foundation. The maximum value of this force is shown to be -0.38×10^6 lb, which means that each anchor bolt is subjected to a tensile force of 95,000 lb. This is greater than the yield force of the bolt (94,248 lb).

The accelerations of the crown and the bed are shown in Figure 29 as functions of the foundation mass. The accelerations of the bed are higher than those at the crown, again due to the fact that the crown has a larger mass than does the bed. The maximum value at the bed is 25.2 g, at a mass ratio of $\alpha = 1$. This value approaches 18 g as the mass ratio increases. The acceleration at the crown is not as dependent on the mass ratio as is that at the bed, since the foundation is coupled to the bed. As the value of α increases above two, the accelerations do not vary to any great degree.

The velocity of the foundation decreases very rapidly as the mass ratio increases in the range where α is less than two. Further increasing the mass, however, hardly affects the velocity, as can be seen in Figure 30.

Dynamic forces transmitted to the foundation are shown in Figure 31 as a function of the mass ratio. These compressive and tensile forces between the press's feet and the foundation result from the relative motion between the bed and the foundation. The transmitted forces are a well

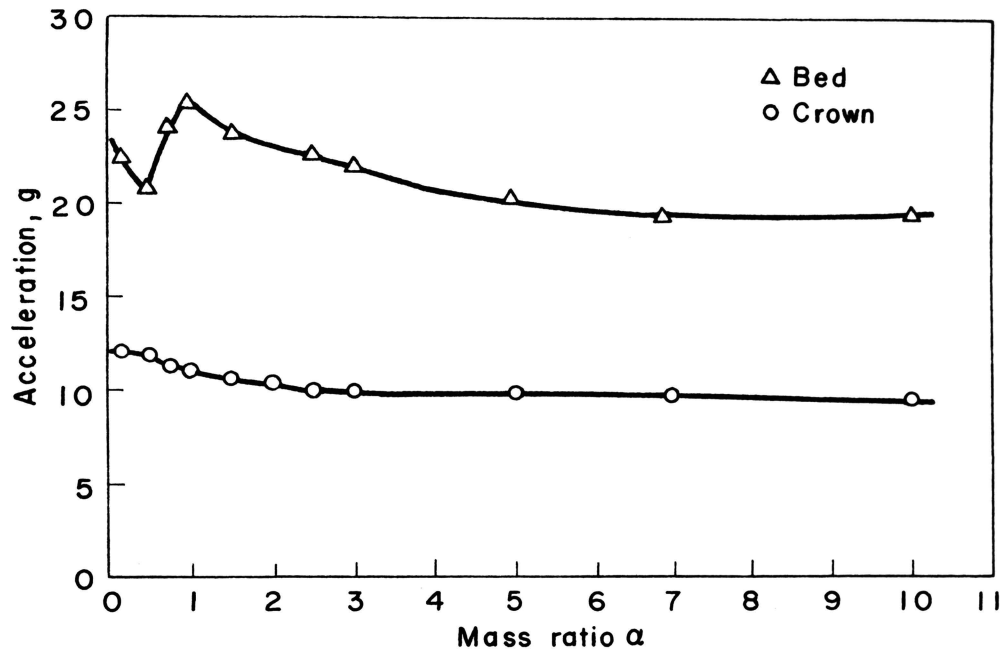


Figure 29. Maximum Acceleration of a Bolted Press as a Function of Foundation Mass

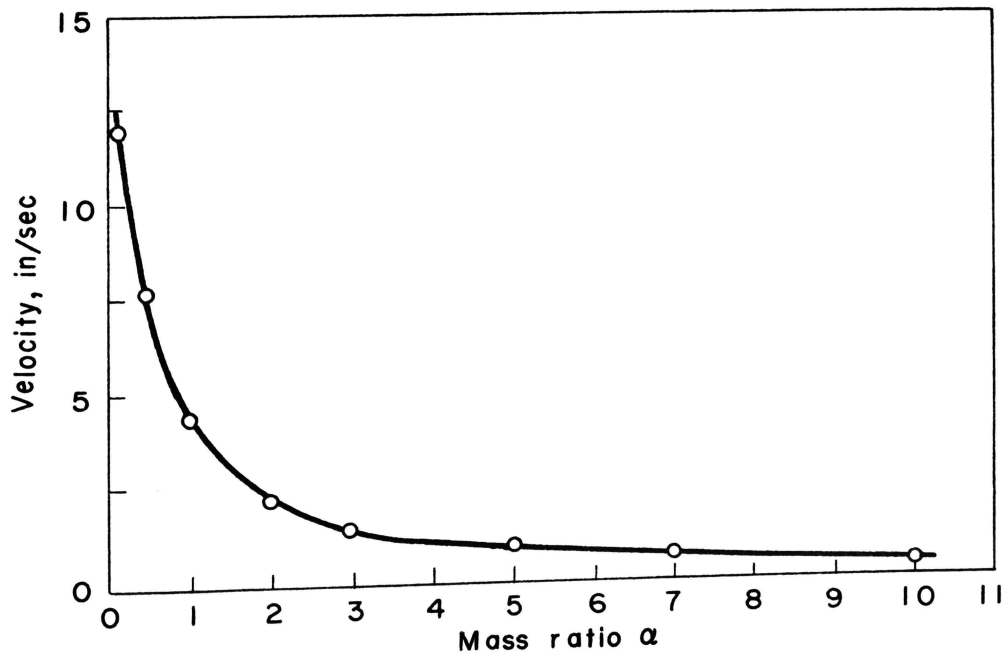


Figure 30. Maximum Velocity of a Bolted Press as a Function of Foundation Mass

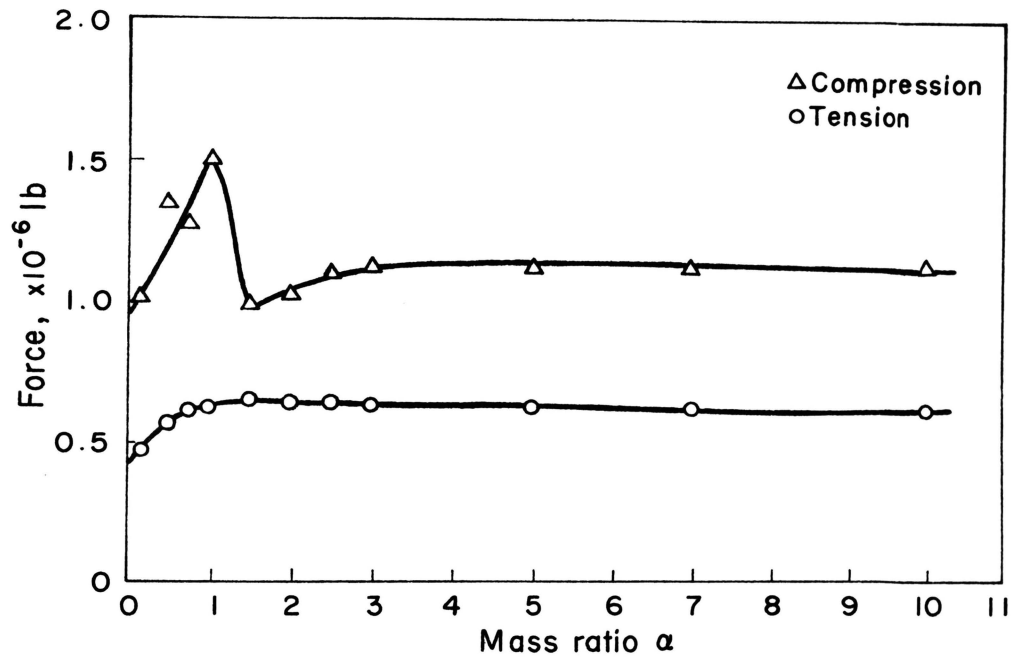


Figure 31. Maximum Dynamic Force Transmitted to the Foundation of a Bolted Press as a Function of Foundation Mass

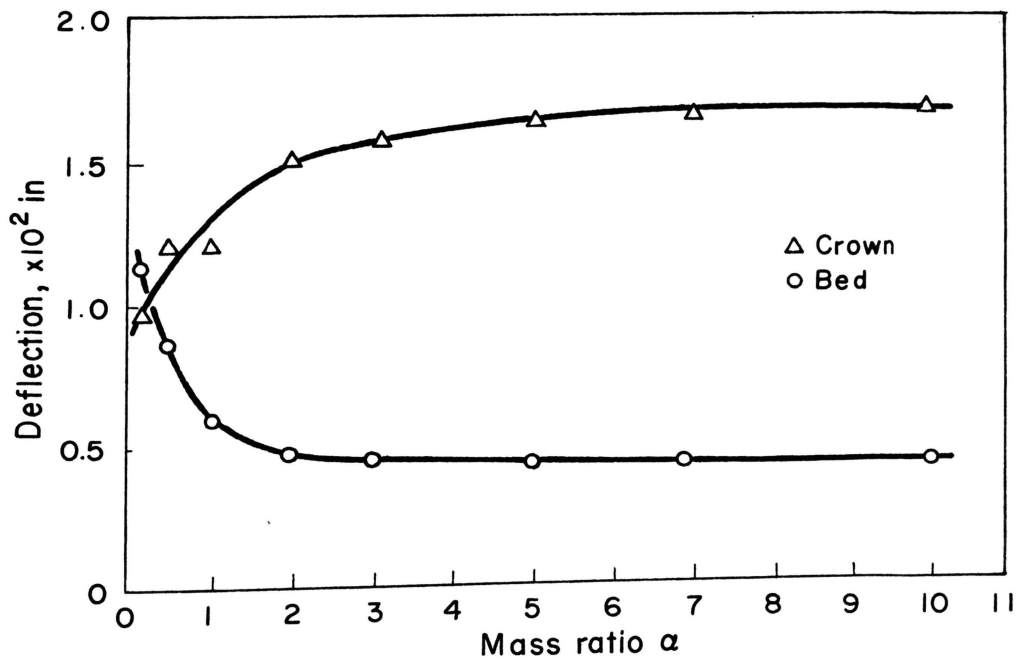


Figure 32. Maximum Deflection of a Bolted Press as a Function of Foundation Mass

known source of numerous problems, such as damage to the foundation, the floor, the walls, and the building structure, as well as to the press and its operators. The maximum and minimum values occur near the mass ratio $\alpha = 1$, where the system is reacting to the dynamic loading. The tensile forces which commonly cause the anchor bolts to break do not vary as the compressive forces do, but their magnitudes explain that breakage problem. These forces are not affected by a mass ratio beyond $\alpha = 2$.

Maximum deflections of the crown and the bed during stamping are plotted and shown in Figure 32 as a function of the mass ratio, α . As the mass ratio increases, the deflection of the bed decreases while that of the crown increases at an equal rate. The maximum relative displacement between the crown and the bed is relatively independent of the mass ratio, while the maximum deflections of the crown and bed are not affected by a mass ratio greater than two.

B. The Effects of Loosened Anchor Bolts

For this phase of the study, it is assumed that the four anchor bolts with which the press has been fastened to its foundation have become loosened, so that there is a clearance of 0.01 inch between each of the press's feet and the bolt head. The stiffness of the combination of loosened anchor bolts and the effective concrete under the

press's feet is shown in Figure 5(b). In the curve, the upper break point is a function of the bolt's clearance.

The accelerations of the crown and the bed are shown in Figure 33 as functions of the foundation mass. The accelerations of the bed are higher than those of the crown, as in the case of the bolted press. The two curves in the figure are also similar to those found in the case of the bolted press, except that the values are slightly lower.

The velocity of the foundation decreases very rapidly as the mass ratio increases, in the range where α is less than two. Further increasing the mass ratio hardly affects the velocity, as can be seen in Figure 34. The curve in this figure is again very similar to the one in the case of the bolted press.

Dynamic forces transmitted to the foundation are shown in Figure 35 as a function of the mass ratio. The upper and lower curves represent compressive and tensile forces, respectively. The average values of the upper and lower curves are calculated to be 1.0×10^6 lb and 0.4×10^6 lb, respectively. These values are lower than those found in the case of the bolted press (1.15×10^6 lb and 0.6×10^6 lb), which is due to the fact that the clearances of the anchor bolts cause the stiffness between the bed and the foundation to be softer than is true for the case of the bolted press.

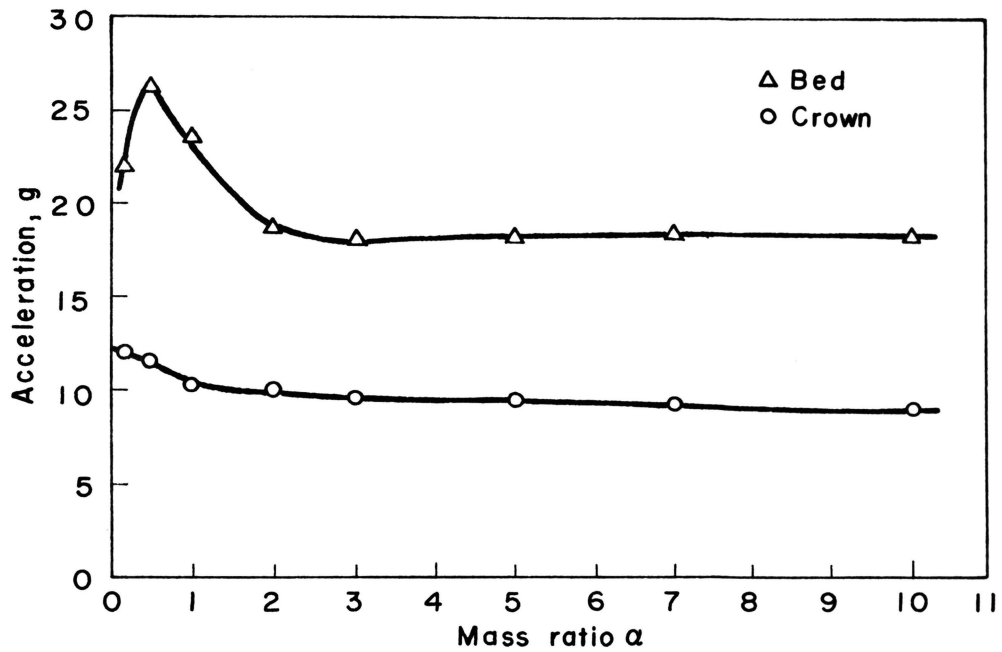


Figure 33. Maximum Acceleration of a Press with Loosened Anchor Bolts as a Function of Foundation Mass

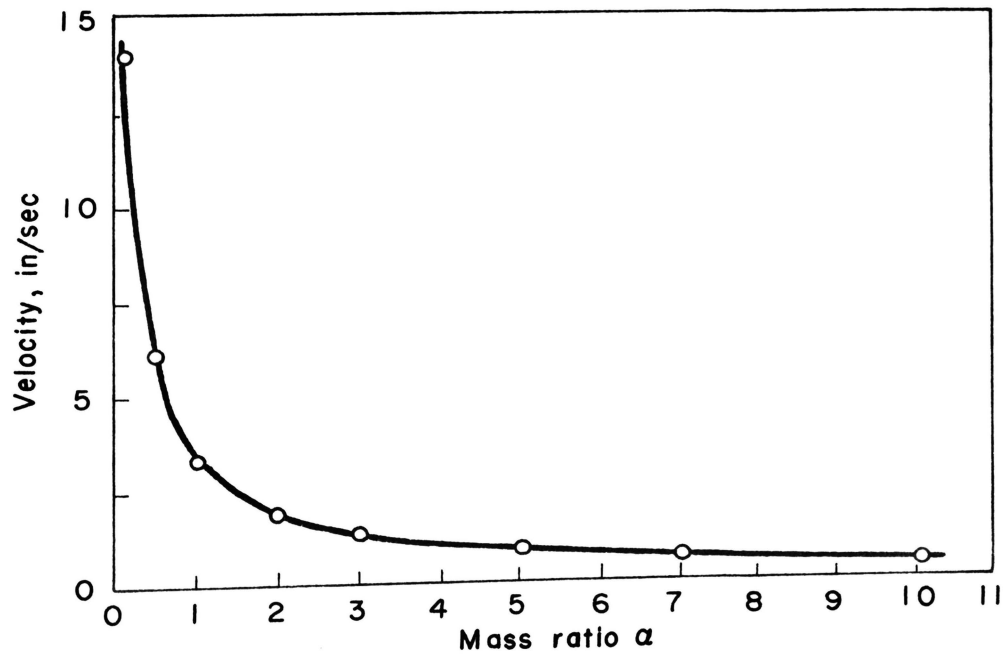


Figure 34. Maximum Foundation Velocity of a Press with Loosened Anchor Bolts as a Function of Foundation Mass

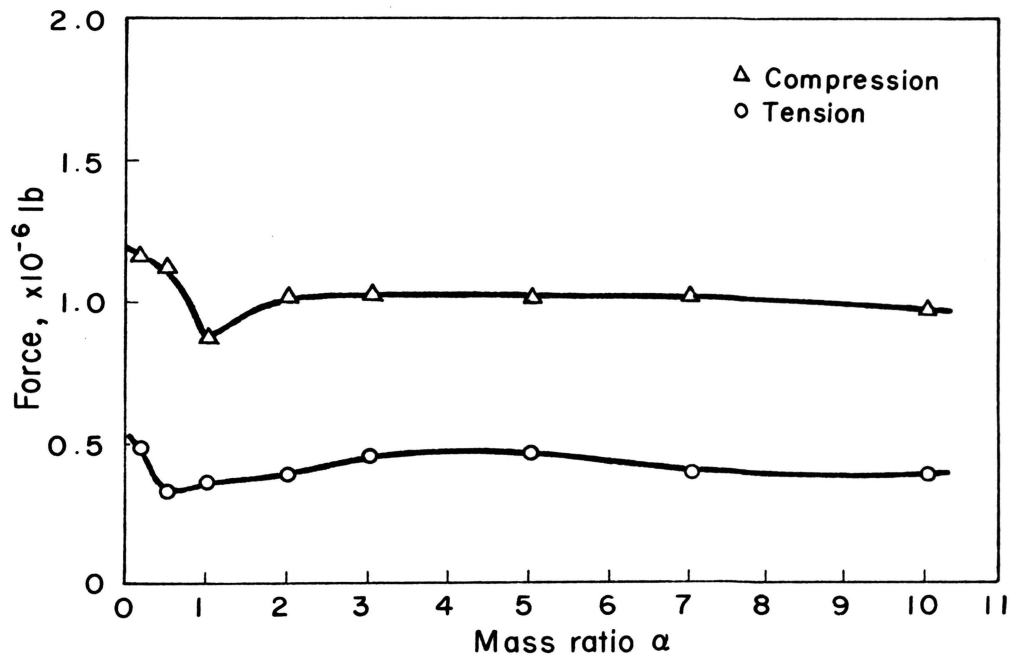


Figure 35. Maximum Dynamic Force Transmitted to the Foundation of a Press with Loosened Anchor Bolts as a Function of Foundation Mass

C. The Effects of Varying the Foundation Mass of a Press Resting on Isolators

Finally, the press is simulated as if mounted on four isolators which sit on a foundation block. Four sets of isolators (7, 15, 25, and 40 Hz) are used to study the specific performance of an isolated press.

The displacements and accelerations of the crown and bed, and the velocity of the foundation versus time are shown in Figures 36, 37, 38, 39, and 40. For this particular simulation, 7 Hz isolators and a mass ratio of $\alpha = 0.5$ are used. The press frequency of 1 Hz, showing its overall resemblance to a cosine curve, is illustrated in Figures 36 and 37.

The frequencies of the crown and the bed are calculated from Figures 36 and 37 to be 136 Hz. The force transmitted to the foundation versus time is shown in Figure 41. The maximum dynamic load is calculated to be 0.038×10^6 lb, which is 0.2 times the static weight of the press. No tensile force transmitted to the foundation is shown, since there is no positive relative displacement between the bed and the foundation.

Accelerations at the crown and the bed are shown in Figure 42 as functions of the mass ratio, α , with the four different sets of isolators. The highest level of acceleration results from the softest isolator (7 Hz). However, the softest isolator also results in an independence of the

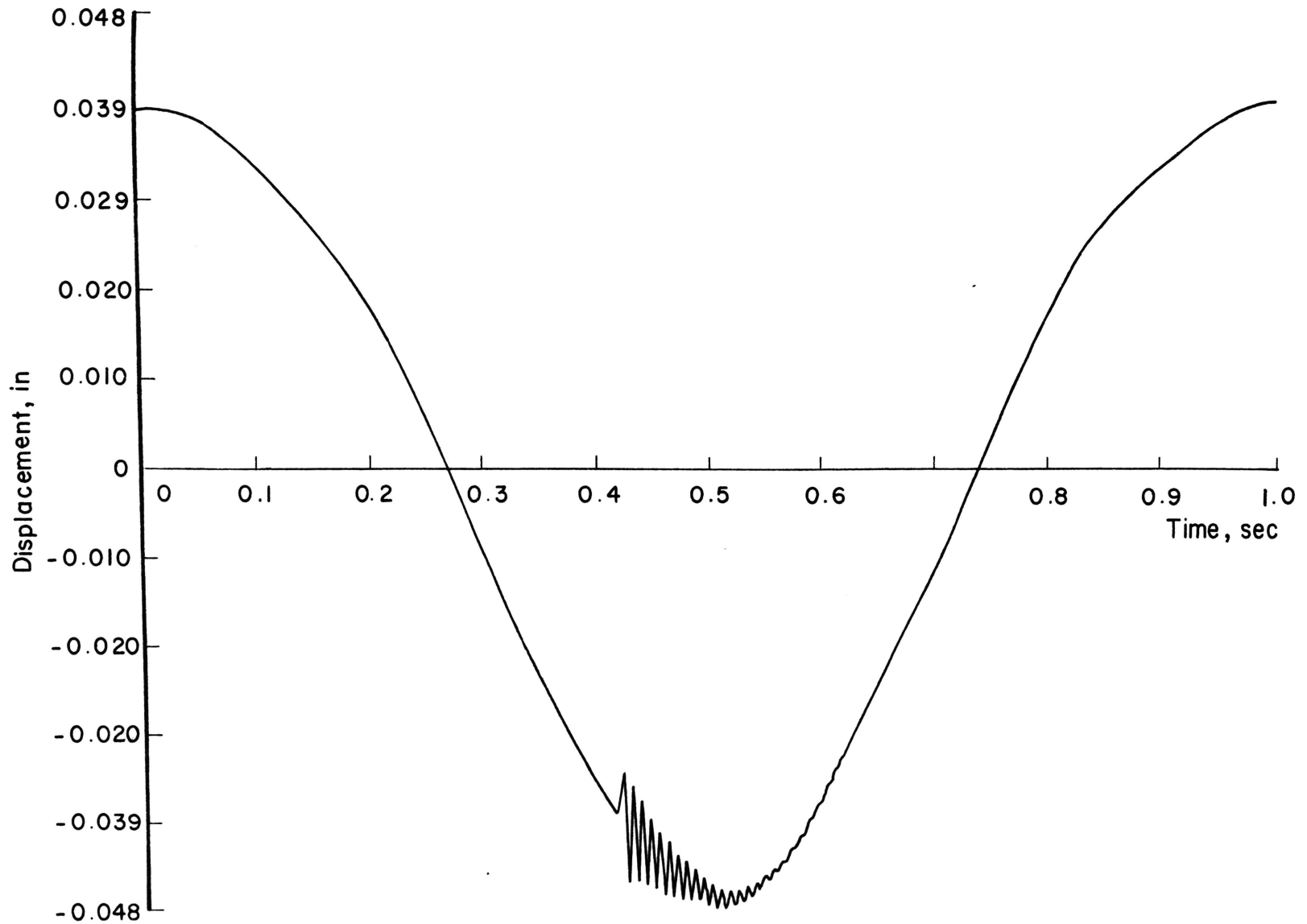


Figure 36. Simulation of an Isolated Press Showing Crown Displacement

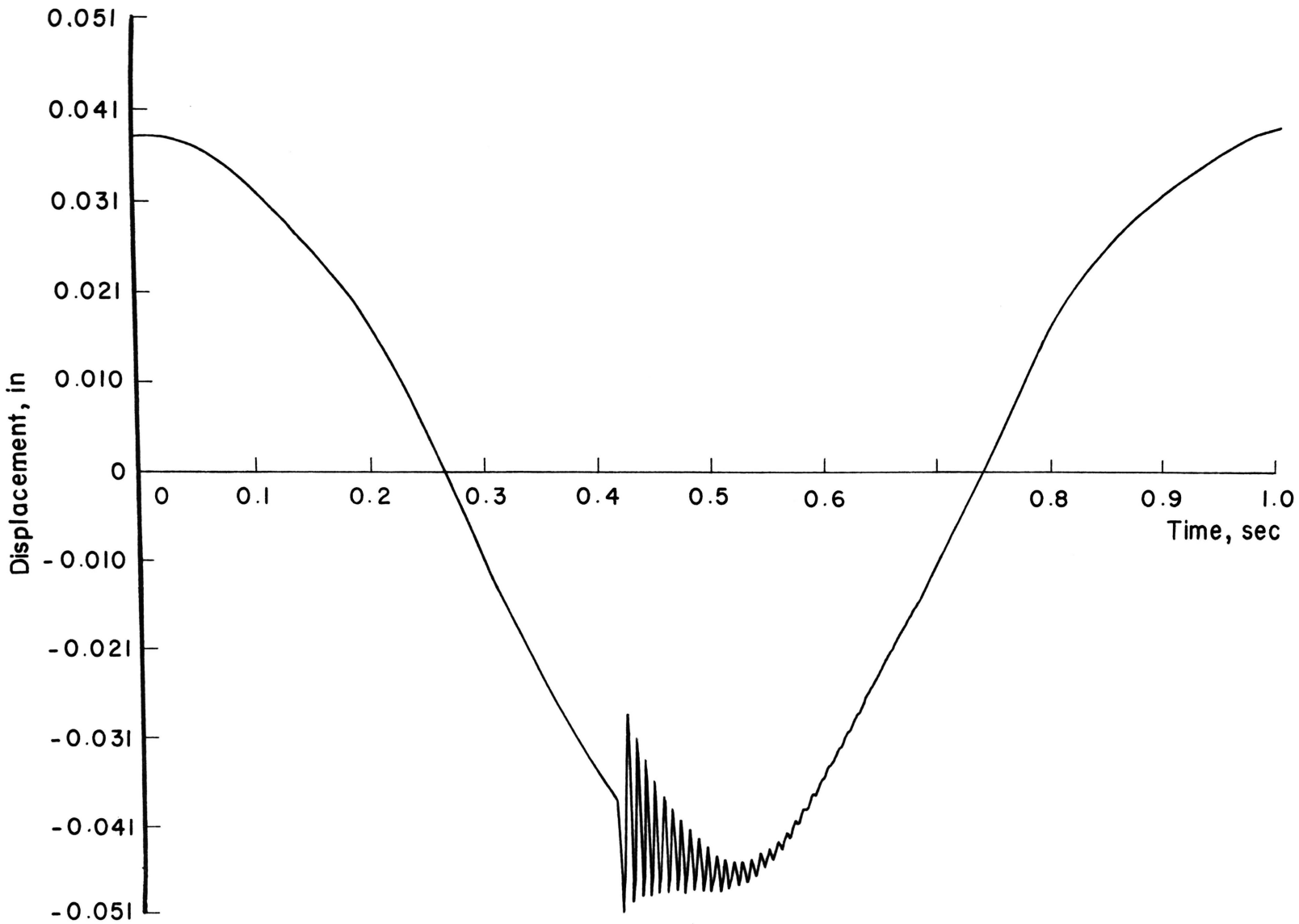


Figure 37. Simulation of an Isolated Press Showing Bed Displacement

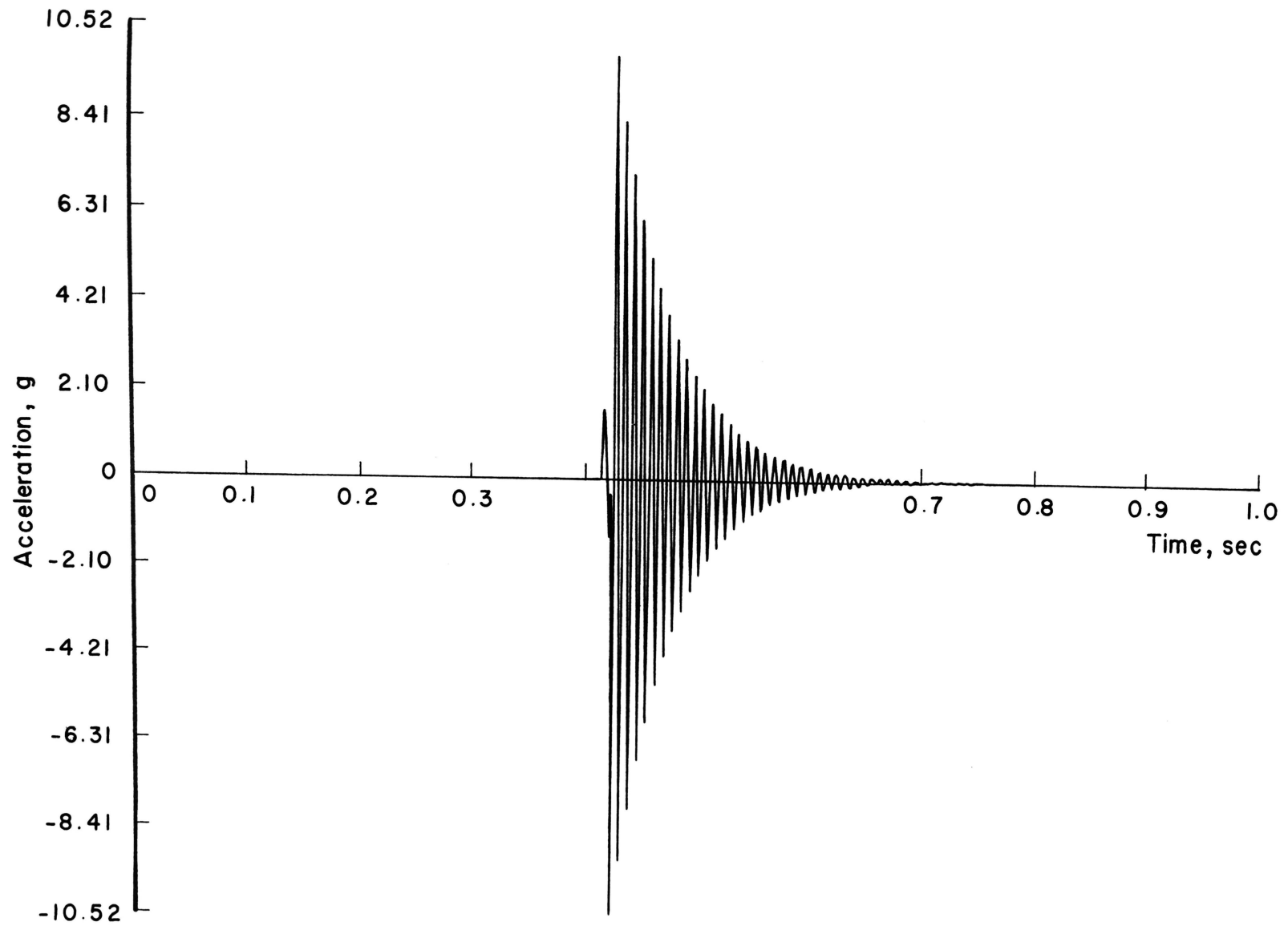


Figure 38. Simulation of an Isolated Press Showing Crown Acceleration

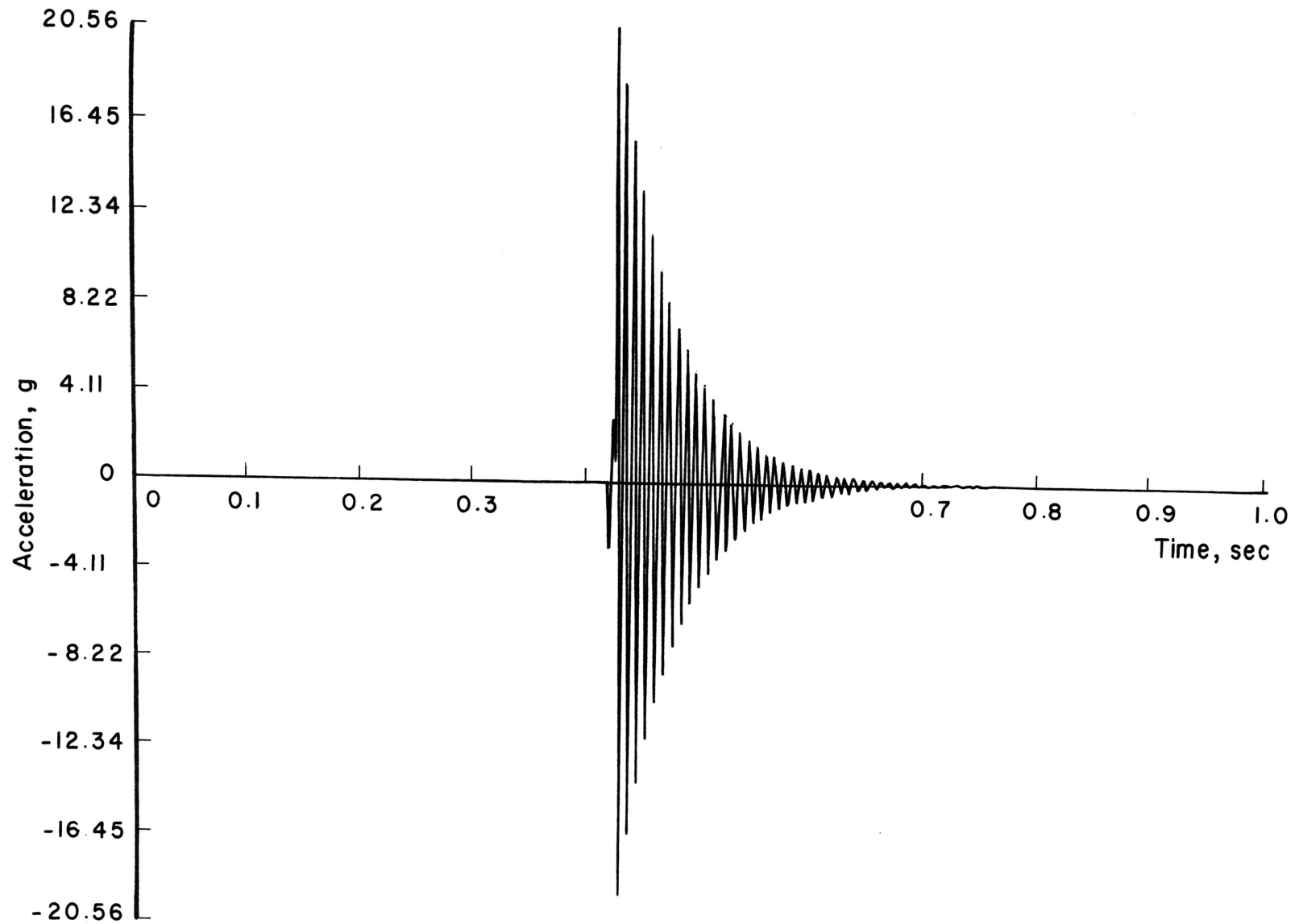


Figure 39. Simulation of an Isolated Press Showing Bed Acceleration

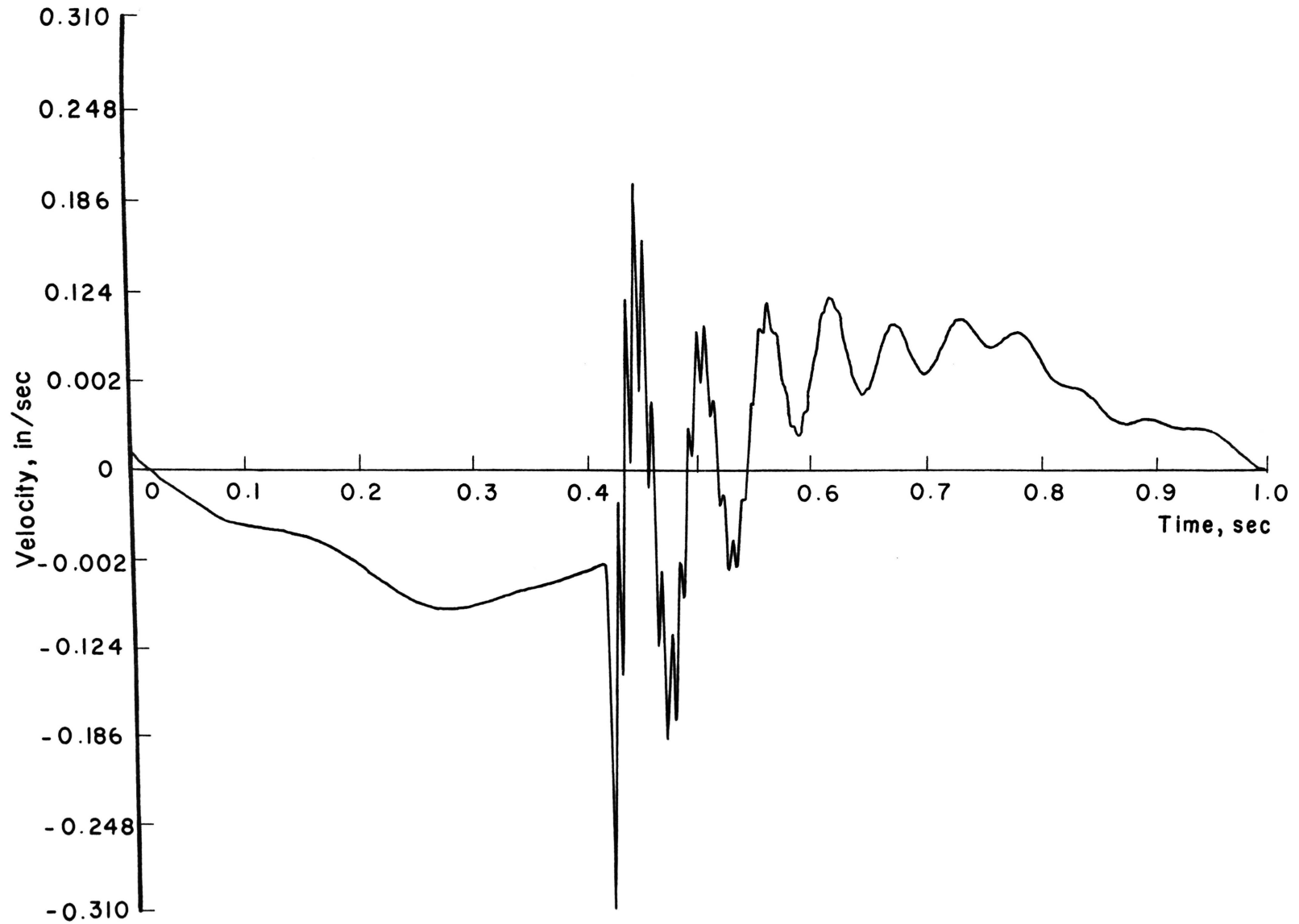


Figure 40. Simulation of an Isolated Press Showing Foundation Velocity

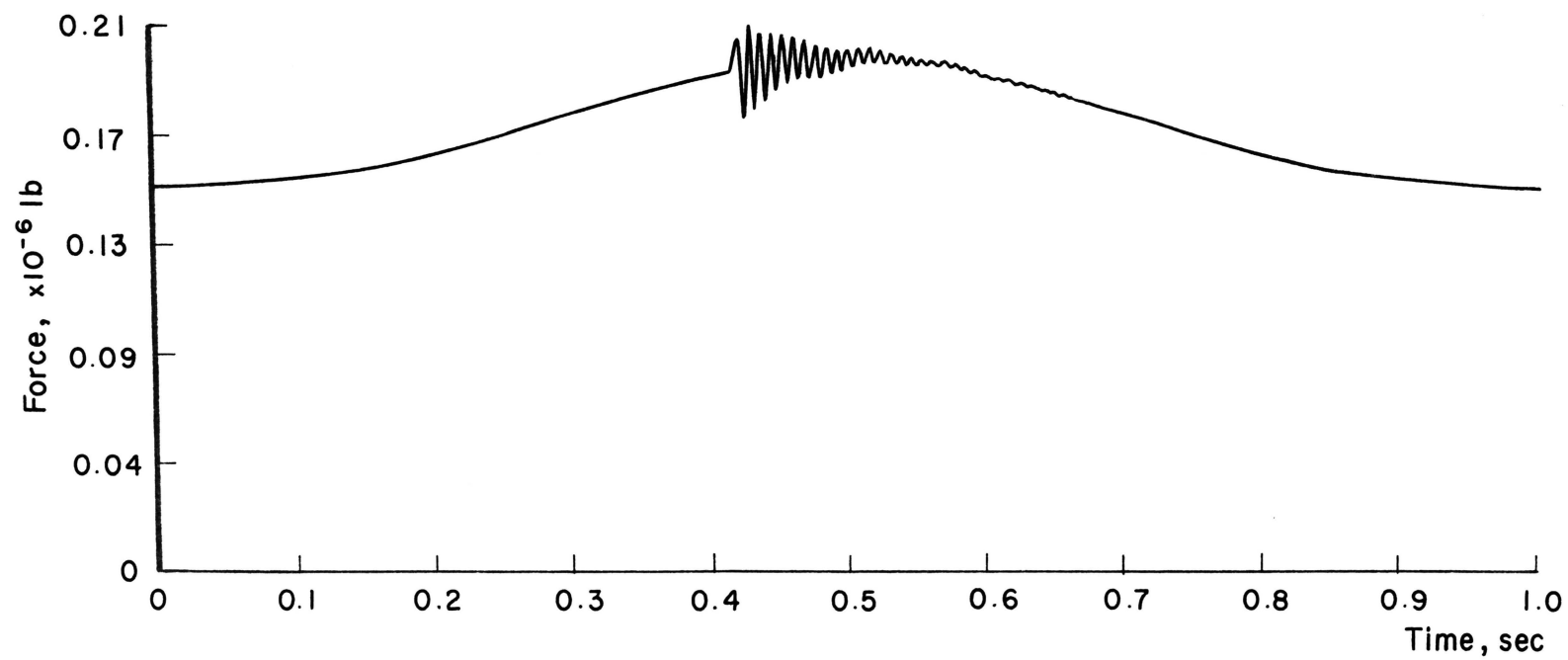


Figure 41. Simulation of an Isolated Press Showing Force Transmitted to the Foundation

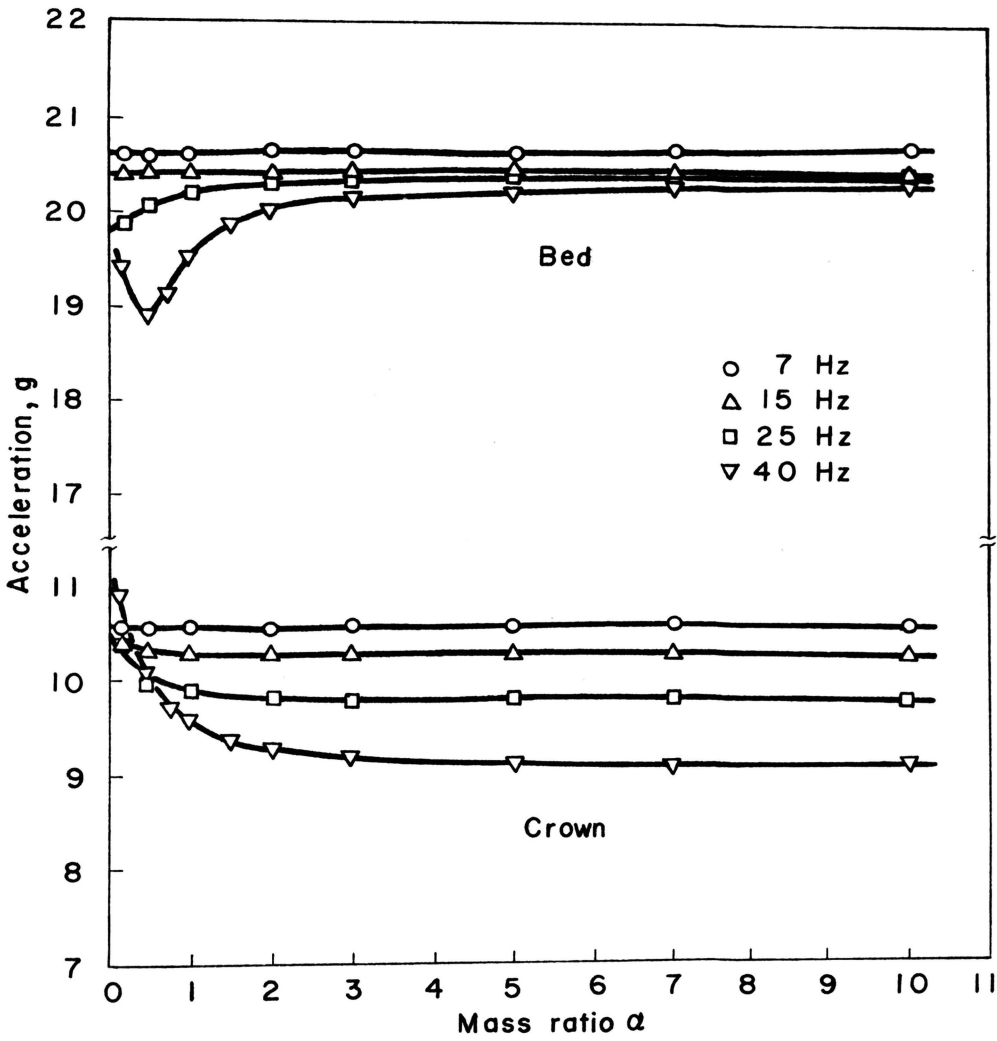


Figure 42. Maximum Acceleration of an Isolated Press as a Function of Foundation Mass

accelerations and the mass ratio. Mass ratios greater than $\alpha = 2$ do not affect the acceleration level.

The velocity of the foundation with the four different sets of isolators is shown in Figure 43 as a function of α . The velocity decreases very rapidly as the mass ratio increases in the range of α less than two. The lowest velocity results from the softest isolator among the four sets. Thus, a soft isolator is superior to a stiffer one in terms of the velocity of the foundation, but it is inferior in that it results in higher accelerations at the crown and bed, as was shown in Figure 42.

Dynamic forces transmitted to the foundation are shown in Figure 44 as a function of the mass ratio for the four different isolators. As the frequency of the isolator is increased, higher transmitted forces and more dynamic reactions result for α less than 1.5. The lowest value of the force results from the softest isolator (7 Hz), and is independent of the mass ratio.

Increasing the frequency of the isolator causes a reduction in the accelerations at the crown and bed. However, increasing this frequency also causes an increase in the foundation velocity and the dynamic forces transmitted to the foundation. Thus, it cannot be concluded that the performance of a press is improved by a reduction in the level of accelerations at the crown and bed alone. The

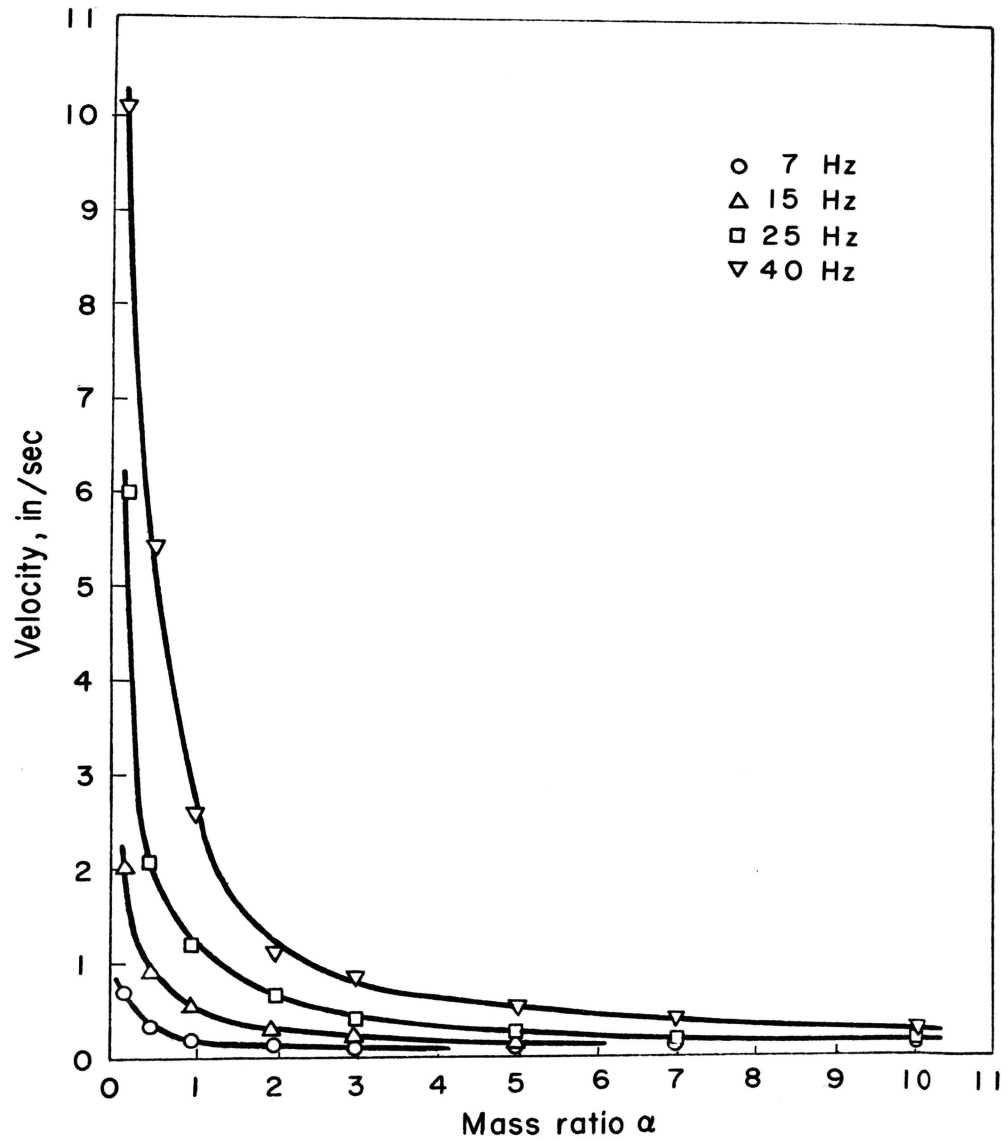


Figure 43. Maximum Foundation Velocity of an Isolated Press as a Function of Foundation Mass

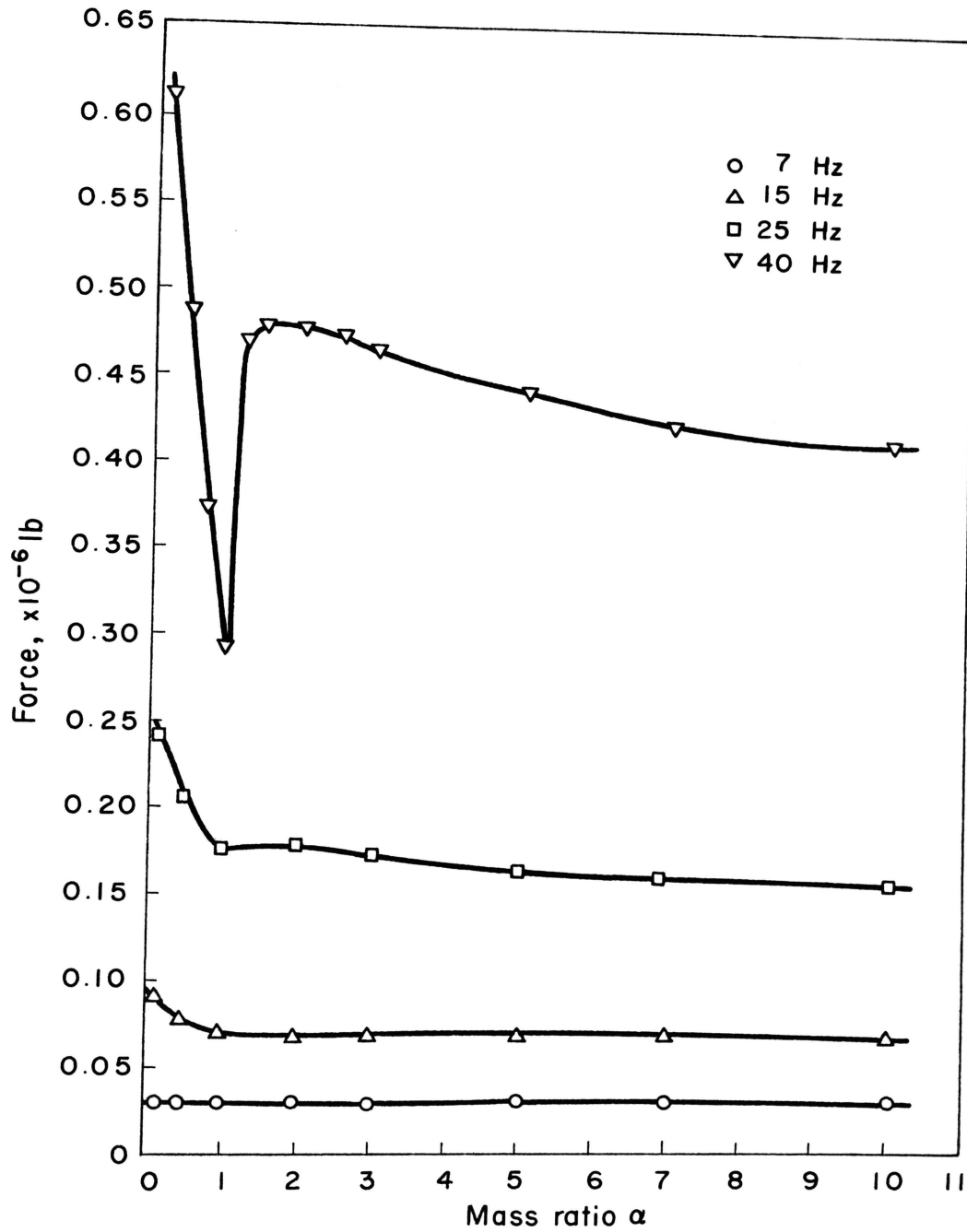


Figure 44. Maximum Dynamic Force Transmitted to the Foundation of an Isolated Press as a Function of Foundation Mass

performance of a press must be discussed in terms of all the possible parameters.

VI. RESULTS AND DISCUSSION

A simplified mathematical model of a press has been formulated and simulated with a computer. Experimental tests were then conducted in order to check the validity of that mathematical model. The following comparisons can be made between the data obtained from those two sources.

- 1) The accelerations of the bed are higher than those of the crown in both the experimental results and the computer simulation results.
- 2) The actual values obtained for the accelerations of the crown and the bed by the experimental tests are similar to those generated by the computer simulation. For the crown, the computer simulation gave a value of 8.0 g, while the experimental values averaged 9.1 g (actual measurements were 8.9 g, 8.0 g, and 10.3 g), representing a variance of about 12 percent. For the bed, the computer simulation value was 13.5 and the experimental measurements averaged 13.3 g (actual values were 13.0 g and 13.6 g), representing a variance of less than two percent.
- 3) The computer simulation shows frequency oscillations, corresponding to the mode in which the crown and bed move in opposition to each other, of 421 Hz. The experimental measurements yield a frequency of 470 Hz, calculated from the acceleration curve of the bed, and

corresponding to a 471 Hz value which is one of the four major frequencies in the spectrum obtained using the fast Fourier transform. Thus, a difference of about eleven percent exists between the computer simulation value and the experimental measurements.

For the first two comparisons, the experimental values used were those measured near the side frames, rather than at the center of the crown and bed. This is because the bending effects of the crown and bed frames tend to amplify the accelerations measured in the center.

This verification of the mathematical model by means of experimental tests permits the continued study of the vertical motion of a press with reasonable confidence in the accuracy of the simulation.

Acceleration of the press, velocity of the foundation, and dynamic forces transmitted to the foundation are all functions of the mass ratio, α , when it is in the range less than two. However, these parameters are relatively independent of the mass ratio when it is greater than two. This phenomenon has been observed in each of the three cases studied: a bolted press, a press with loosened anchor bolts, and an isolated press. Thus, it follows that the performance of a press is not certain to improve when the foundation mass is increased above α greater than two, at the range of α where the dynamic reaction occurs.

There is no noticeable difference in the performance of a bolted press and one with loosened bolts. In the latter case, the acceleration of the press, the velocity of the foundation, and the dynamic force transmitted to the foundation are all slightly less than in the case of a bolted press. This result is due to the fact that the clearance of the anchor bolts causes the stiffness between the bed and the foundation to be softer than it is with a bolted press.

There are, however, significant differences between the performance of a bolted press and that of an isolated press. The latter shows approximately five percent higher acceleration of its crown and bed than does the bolted press. But the isolated press shows a significant superiority over the bolted press in four areas.

- a) The force transmitted to the foundation of an isolated press is 94 percent less than that transmitted to the foundation of a bolted press.
 - b) The velocity of the foundation of an isolated press is 97 percent less than that of a bolted press.
 - c) No tensile force is transmitted to the foundation of an isolated press.
 - d) Higher frequency oscillations are observed in the bed of a bolted press than in the bed of an isolated press.
- These high levels of transmitted forces, velocity, and high frequency oscillations are well known sources of

numerous problems, such as damage to the foundation (including settling), the floor, the walls, and the building structures, as well as to the press and its operators.

In this particular case, a relatively simple measurement of acceleration would imply that a bolted press performs better than an isolated one. More detailed study, however, has revealed that in four other important areas the isolated press is superior. Thus, it is important that as many parameters as possible be considered when evaluating the performance of a press.

VII. CONCLUSIONS AND RECOMMENDATIONS

A method for understanding and studying the dynamic response of a press with a straight-sided frame has been developed by means of computer simulations of a mathematical model for vertical motion. It provides a fundamental approach to the solution of press problems, while the trial and error method which is often used (10) can give only a localized view. The mathematical expression of the press's motion was based on the assumption that the vertical component of motion is the primary source of the dynamic excitation which affects the operator, nearby equipment, and the building.

The simulations show that the overall performance of an isolated press is superior to that of a bolted one. They further indicate that press performance is a function of foundation mass when it is less than approximately twice the mass of the press. Increasing the foundation mass above this ratio did not significantly affect the performance of a bolted press, of one with loosened anchor bolts, or of an isolated press. Thus, the degree of improvement in a press's performance obtained by increasing the mass of its foundation to more than twice that of the press itself is not sufficient to justify the economic investment required.

Horizontal and rotational motions of a press, as well as their interactions with each other and with the vertical motion, remain to be studied by means of a mathematical model. Such interesting phenomena as "press walking" could be analyzed and solved by this method. The modified model would be suitable for studying an inclined press, where the horizontal and rotational motions are important, and depend on the inclination angle as well as the loading conditions. Further extensions would include high speed presses (1500 strokes per minute), where inertial forces play a vital role. Finally, the effects of the drive train itself could be included to make the model more complete.

BIBLIOGRAPHY

1. Crocker, Malcolm J. "Industrial Noise Criteria and Control," in Noise and Vibration Control Engineering, ed. M. J. Crocker, Proceedings of the Purdue Noise Control Conference, Purdue University, Lafayette, Indiana, July 14-16, 1971, 132f.
2. Shinaishin, O. A. "On Punch Press Diagnostics and Noise Control," Inter-Noise '72 Proceedings, Washington, D.C., October 4-6, 1972, 243f.
3. Ruzicka, Jerome E. "Fundamental Concepts of Vibration Control," in Noise and Vibration Control Engineering, ed. M. J. Crocker, Proceedings of the Purdue Noise Control Conference, Purdue University, Lafayette, Indiana, July 14-16, 1971, 170f.
4. Young, Sheldon E. "Controlling Vibration and Structure-Borne Noise through Improved Press Installation," presented at the General Motors Power Press Noise Control Conference, March 6-7, 1974.
5. Miller, H. Timothy "Practical Design of Machinery Foundations for Vibration and Noise Control," Inter-Noise '72 Proceedings, Washington, D.C., October 4-6, 1972, 185f.
6. Barkan, D. D. Dynamics of Bases and Foundations. New York: McGraw-Hill, 1962.
7. Eary, Donald F., and E. A. Reed. Techniques of Pressworking Sheet Metal, 2nd Edition. Englewood Cliffs: Prentice-Hall, 1974.
8. Richart, F. E., Jr., and others. Vibrations of Soils and Foundations. Englewood Cliffs: Prentice-Hall, 1970.
9. System/360 Scientific Subroutine Package, (360A-CM-03X) Version III, Programmer's Manual, IBM Technical Publications Dept., White Plains, N.Y., 1968.
10. Holben, Tod "Trial and Error with Production Presses," presented at Topics in Noise Control Seminar, Engineers' Club and Midwest Noise Council, St. Louis, Missouri, May 14, 1974.

VITA

Woosoon Bai was born on February 2, 1940, in Korea. He received his primary and secondary education in Seoul, Korea, and a Bachelor of Science Degree from the Department of Mechanical Engineering at In-Ha Institute of Technology in December 1964, in Inchon, Korea.

Mr. Bai has been enrolled in the Graduate School of the University of Missouri - Rolla since September 1968, and received his Masters Degree from the Department of Engineering Mechanics at that institution in December 1970. He was associated with the Rock Mechanics and Explosives Research Center as a graduate research assistant from September 1969 through December 1972.

APPENDIX A

Table 1. Specifications of the 60 Ton Press

	WEIGHT*	LENGTH	DIAMETER	AREA	STIFFNESS	DAMPING COEFF.	DAMPING RATIO
	(lb)	(in)	(in)	(in ²)	(lb/in)	(lb/in/sec)	(c/cc)
CROWN	7075.	--	--	--	--	--	--
BED	5015.	--	--	--	--	--	--
SLIDE	1410.	--	--	--	--	--	--
FOUNDATION	8100.**	--	--	5425.	--	--	--
CRANK ARM	--	3.00	--	--	--	--	--
CONNECTING ROD	--	15.12	3.13	7.64	--	--	--
TIE ROD	--	82.25	2.50	--	1.75×10^6	1.93×10^2	0.007
COLUMN	--	47.50	--	18.15	1.15×10^7	1.93×10^2	0.007
SOIL	--	--	--	--	7.9×10^5	2.53×10	0.010
ISOLATOR	--	(9.9 Hz)	--	--	3.40×10^4	6.88×10	0.050

* Estimated values

** Depending on mass ratio α , for this example, $\alpha = 0.6$

APPENDIX B

Table 2. Specifications of the 600 Ton Press

	WEIGHT*	LENGTH	DIAMETER	AREA	STIFFNESS	DAMPING COEFF.	DAMPING RATIO
	(lb)	(in)	(in)	(in ²)	(lb/in)	(lb/in/sec)	(c/cc)
CROWN	67062	--	--	--	--	--	--
BED	58142	--	--	--	--	--	--
SLIDE	46000	--	--	--	--	--	--
FOUNDATION	85600**	--	--	--	--	--	--
CRANK ARM	--	10.	--	--	--	--	--
CONNECTING ROD	--	53.25	--	--	--	--	--
TIE ROD	--	244.	6.50	--	4.08×10^6	1.01×10^2	0.001
COLUMN	--	113.75	--	45.75	1.12×10^7	1.01×10^2	0.001
CONCRETE	--	--	--	--	1.75×10^7	4.62×10^2	0.010
SOIL**	--	--	--	--	1.77×10^6	2.51×10^3	0.10
ANCHOR BOLT	--	27.	2.00	--	3.49×10^6	9.26×10	0.002
ISOLATOR	--	(7 Hz)	--	--	2.14×10^6	4.26×10^6	0.050

* Estimated values

** Depending on mass ratio α , for this example, $\alpha = 0.5$

243152